Thermal evolution with a hydrating mantle and the initiation of plate tectonics in the early Earth

J. Korenaga[1]

Received 31 March 2011; revised 20 September 2011; accepted 23 September 2011; published 10 December 2011.

[1] The net influx of water into the deep mantle by plate tectonics has been poorly constrained because it is difficult to quantify how efficiently subducting slabs are devolatilized on a global scale. The significance of deep water cycle in the Earth history is similarly ambiguous because it depends critically on when plate tectonics started and how it evolved through time. Here I show that, using the new scaling of plate-tectonic convection based on fully dynamic calculations, the thermal evolution of Earth consistent with geochemical, petrological, and geological data requires continuous mantle hydration since the early Earth, with the net water influx of ~2–3 × 10^{14} g yr^{-1}. A drier mantle in the Hadean and Archean is suggested to help the initiation of plate tectonics by reducing the viscosity contrast between lithosphere and asthenosphere. As an increase in the vigor of plate tectonics with time would encourage global marine inundation, the slow intake of surface water by the convecting mantle is essential to maintain the continental freeboard.

Citation: Korenaga, J. (2011), Thermal evolution with a hydrating mantle and the initiation of plate tectonics in the early Earth, *J. Geophys. Res.*, *116*, B12403, doi:10.1029/2011JB008410.

1. Introduction

[2] Reconstructing the thermal evolution of Earth is one of the most fundamental geophysical problems, providing a global context for a range of geological processes throughout the Earth history. This fundamental nature also makes it difficult to solve because reconstruction must be consistent not only with the physics of Earth's interior but also with a variety of observational constraints, such as geochemical constraints on thermal budget, petrological constraints on secular cooling, and geological constraints on ancient tectonics. Satisfying both of such theoretical and observational requirements has long been a challenge [e.g., *Christensen*, 1985; *Richter*, 1985; *Honda*, 1995; *Solomatov*, 2001; *Korenaga*, 2006]; in particular, elementary fluid mechanics suggests that the vigor of mantle convection would decrease as Earth cools down, but this apparently innocuous behavior of the mantle fails to explain the present-day thermal budget of Earth. It has been suggested that, because of the effect of chemical differentiation on mantle dynamics, plate tectonics may have been more sluggish when the mantle was hotter, and with this inverse relation between internal temperature and the vigor of mantle convection, it is possible to reconstruct a thermal history without violating the thermal budget [*Korenaga*, 2003, 2006]. The suggestion of sluggish plate tectonics was, however, based on the global energy balance assuming the operation of plate tectonics in the past. This points to another long-standing question: When did plate tectonics start on Earth? [e.g., *Condie and Pease*, 2008]. As different modes of mantle convection release heat at different rates [e.g., *Solomatov*, 1995], this question is of critical importance when reconstructing the thermal evolution of Earth over its entire history.

[3] To address these issues, the scaling of mantle convection has recently been derived from a series of numerical simulations with the self-consistent generation of plate tectonics [*Korenaga*, 2010a]. These numerical simulations employ the so-called pseudoplastic rheology introduced by *Moresi and Solomatov* [1998], with strongly temperature-dependent viscosity to make the derived scaling relevant to the real Earth. A criterion for the operation of plate tectonics has also been quantified, and we can now model the thermal evolution of Earth on the basis of fully dynamic simulations and, at the same time, test the assumption of plate tectonics in a quantitative manner. The purpose of this paper is, therefore, to explore the likely thermal evolution of Earth using the new scaling law of mantle convection and evaluate the plausibility of various speculations made in previous studies. The paper is organized as follows. First, the theoretical formulation is described in detail, together with justifications for model setup (section 2). Thermal evolution modeling involves a number of parameters, many of which suffer from nontrivial uncertainties. A Monte Carlo approach is thus adopted to efficiently sample the multidimensional parameter space, and a large number of modeling results are used to delineate the likely evolutionary path (section 3). Two cases of thermal evolution are considered, one with a closed mantle system and the other with a mantle that can exchange water with oceans, and the latter is suggested to be more consistent with available geological data. The possibility of plate tectonics in

[1]Department of Geology and Geophysics, Yale University, New Haven, Connecticut, USA.

0148-0227/11/2011JB008410

Table 1. Radiogenic Heat Production

Isotope	p_n[a] (W/kg)	$c_{m,n}$[b]	$h_{m,n}$	$c_{cc,n}$[c]	$h_{cc,n}$	$\sigma_{1/2}$[a] (Ga)	λ_n[a] (1/Ga)
^{238}U	9.37×10^{-5}	0.9927	0.372	0.9927	0.348	4.47	0.155
^{235}U	5.69×10^{-4}	0.0072	0.0164	0.0072	0.0153	0.704	0.985
^{232}Th	2.69×10^{-5}	4.0	0.430	5.0	0.503	14.0	0.0495
^{40}K	2.79×10^{-5}	1.6256	0.181	1.28	0.134	1.25	0.555

[a]From *Turcotte and Schubert* [1982].
[b]Relative concentration normalized by the abundance of total U, with U:Th:K = 1:4:(1.27 × 10^4), ^{238}U/U = 0.9927, ^{235}U/U = 0.0072, and ^{40}K/K = 1.28 × 10^{-4}. All Th is ^{232}Th.
[c]Same as previous, but with U:Th:K = 1:5:10^4.

the early Earth is then discussed, along with its connection to global water cycle (section 4).

2. Theoretical Formulation

2.1. Global Heat Balance

[4] To reconstruct a thermal history of Earth, the following global energy balance [e.g., *Christensen*, 1985] is integrated backward in time starting from the present-day,

$$C\frac{dT_p(t)}{dt} = H(t) - Q(t), \tag{1}$$

where C is the heat capacity of the entire Earth (~7 × 10^{27} J K^{-1}), T_p is the mantle potential temperature (a hypothetical temperature of the mantle adiabatically brought up to the surface without melting), t is time, H is the internal heat production in the mantle, and Q is surface heat flux by mantle convection. In all models in this study, the present-day potential temperature $T_p(0)$ is set to 1350°C [*Herzberg et al.*, 2007]. This equation assumes that the temperature contrast between the mantle and the core is constant through time [*Korenaga*, 2008b, section 3.5], i.e., core heat flux is proportional to the secular cooling of the mantle. The detail of core heat flux parameterization is important for the thermal history of the core, but not for that of the mantle [*Korenaga*, 2008c], so equation (1) is sufficient for this study.

[5] Backward integration is preferred over forward integration for the following two reasons. First, it is better to use the present-day, which is the best understood part of the Earth history, as an initial condition. Second, my modeling strategy is to assume mantle convection to be in the mode of plate tectonics throughout the Earth history and test the validity of this assumption afterwards. Backward integration is suitable for this strategy because, even when the operation of plate tectonics cannot be justified at some point in the history, modeling results will still be useful up to then.

[6] As long as $H(t)$ and $Q(t)$ are well defined, the numerical integration of equation (1) is computationally trivial, and the calculation of the mantle heat production $H(t)$ is straightforward (section 2.2). Calculating the mantle heat flux $Q(t)$ is, however, much more involved (section 2.3), and in fact, how to parameterize this heat flux constitutes the essence of thermal evolution modeling.

2.2. Mantle Heat Production

[7] Mantle heat production at the present-day, $H_m(0)$, may be estimated as the difference between the heat production of the bulk silicate Earth (BSE), 16 ± 3 TW [*Lyubetskaya and Korenaga*, 2007b], and that of continental crust, 7.5 ± 2.5 TW [*Rudnick and Gao*, 2004], as

$$H_m(0) = 16 - H_{cc}(0) + 3\varepsilon_1[\mathrm{TW}], \tag{2}$$

where $H_{cc}(0)$ is the present-day heat production in the continental crust as

$$H_{cc}(0) = 7.5 + 2.5\varepsilon_2[\mathrm{TW}], \tag{3}$$

and ε_i's are independent random variables with zero mean and unit standard deviation. The use of two independent random variables is to signify that the uncertainty of the BSE heat production is uncorrelated with that of the continental heat production. Once these present-day values are specified, their values in the past can be backtracked as

$$H_i(t) = H_i(0)\sum_{n=1}^{4} h_{i,n}\exp(\lambda_n t), \tag{4}$$

where λ_n is the decay constant of n-th radioactive isotope (^{238}U, ^{235}U, ^{232}Th, and ^{40}K), and $h_{i,n}$ is its relative contribution to the total heat production of either mantle ($i = m$) or continental crust ($i = cc$) defined as

$$h_{i,n} = \frac{c_{i,n}p_n}{\sum_n c_{i,n}p_n}. \tag{5}$$

Here the heat generation rates of the radioactive isotopes are denoted by p_n, and their relative concentrations in the i-th reservoir by $c_{i,n}$. Values used for these parameters are given in Table 1.

[8] At the present day, $H(0)$ is equivalent with $H_m(0)$. When the continental mass was smaller in the past, mantle heat production must be correspondingly greater, and the total mantle heat production is calculated as

$$H(t) = H_m(t) + [1 - F_{cc}(t)]H_{cc}(t), \tag{6}$$

where F_{cc} is the mass fraction of continental crust with respect to the present-day value. Continental growth models exhibit considerable variability in the Archean [e.g., *Collerson and Kamber*, 1999; *Campbell*, 2003; *Harrison et al.*, 2005; *Hawkesworth and Kemp*, 2006], so I explore a wide range of possibilities spanning from the instantaneous growth model of *Armstrong* [1981] to the gradual growth model of *McLennan and Taylor* [1982] as

$$F_{cc}(t) = f_{\mathrm{mix}}F^{\mathrm{A}}_{cc}(t) + (1 - f_{\mathrm{mix}})F^{\mathrm{MT}}_{cc}(t), \tag{7}$$

where f_{mix} is a random variable ranging from 0 to 1 (Figure 1).

2.3. Mantle Heat Flux

[9] The mantle heat flux is calculated as

$$Q(t) = \frac{kA\Delta T_p(t)Nu(t)}{D}, \tag{8}$$

where k is thermal conductivity (4 W m^{-1} K^{-1}), A is the surface area of Earth (5.1 × 10^{14} m^2), ΔT_p is the potential temperature difference between the surface and the interior, Nu is the Nusselt number, and D is the mantle depth (2.9 × 10^6 m). For plate-tectonic convection with pseudoplastic

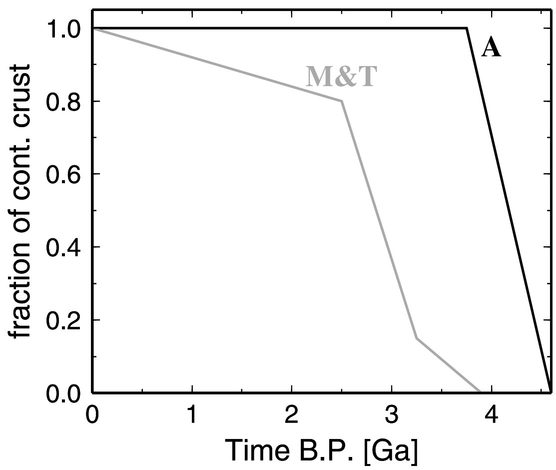

Figure 1. Two end-member models of continental growth used in thermal evolution modeling: *Armstrong* [1981] (solid) and *McLennan and Taylor* [1982] (gray).

rheology, the Nusselt number may be calculated as [*Korenaga*, 2010a]

$$Nu(t) = 2\left(\frac{Ra_i(t)}{Ra_c}\right)^{1/3} \Delta\eta_L(t)^{-1/3}, \tag{9}$$

where Ra_i is the internal Rayleigh number, Ra_c is the critical Rayleigh number ($\equiv 10^3$), and $\Delta\eta_L$ is the lithospheric viscosity contrast. The internal Rayleigh number is defined as

$$Ra_i(t) = \frac{\alpha\rho g \Delta T_p(t) D^3}{\kappa \eta_i(T_p(t))}, \tag{10}$$

where α is thermal expansivity (2×10^{-5} K^{-1}), ρ is mantle density (4000 kg m^{-3}), g is gravitational acceleration (9.8 m s^{-2}), κ is thermal diffusivity (10^{-6} m^2 s^{-1}), and η_i is the interior viscosity, the temperature dependency of which is specified as

$$\eta_i(T_p(t)) = \eta_r \exp\left[\frac{E}{R(T_p(t))} - \frac{E}{R(T_p(0))}\right]. \tag{11}$$

Here E is the activation energy, R is the universal gas constant, and η_r is the reference viscosity at $T_p = T_p(0)$.

[10] When mantle rheology is controlled by the above temperature-dependent viscosity as well as the brittle failure criterion (i.e., pseudoplastic rheology), the lithospheric viscosity contrast in equation (9) may be parameterized as [*Korenaga*, 2010a]

$$\Delta\eta_L(\gamma, \theta) \approx \exp(0.327\gamma^{0.647}\theta), \tag{12}$$

where γ is a normalized version of an effective friction coefficient μ, defined as

$$\gamma = \frac{\mu}{\alpha \Delta T_p}, \tag{13}$$

and θ is a nondimensional measure of temperature-dependent viscosity defined as

$$\theta = \frac{E\Delta T_p}{RT_p^2}. \tag{14}$$

The critical viscosity contrast above which plate tectonics is dynamically implausible is given by [*Korenaga*, 2010a]

$$\Delta\eta_{L,crit}(t) = 0.25Ra_i(t)^{1/2}. \tag{15}$$

[11] When mantle convection is in the mode of plate tectonics, the mantle melts beneath mid-ocean ridges, and this mantle melting creates a dehydrated lithosphere. As the initial pressure of melting (in GPa) for dry pyrolitic mantle is given by [*Takahashi and Kushiro*, 1983]

$$P_o = (T_p - 1423)/100, \tag{16}$$

the thickness of the dehydrated lithosphere may be calculated as

$$h_m = \frac{P_o}{\rho g}. \tag{17}$$

Mantle viscosity depends not only on temperature but also on the water content, and a drier mantle is usually stiffer [e.g., *Karato et al.*, 1986; *Hirth and Kohlstedt*, 1996; *Mei and Kohlstedt*, 2000; *Faul and Jackson*, 2007]. Hotter mantle in the past thus results in thicker dehydrated (and thus stiff) lithosphere. *Korenaga* [2010a] found that the effect of viscosity stratification caused by mantle melting may be captured by redefining the lithospheric viscosity contrast as

$$\Delta\eta_L \approx \Delta\eta_{L,\mathrm{ref}} \exp\left[\ln(\Delta\eta)\max\left(1, \frac{h_m}{6h_{\mathrm{ref}}}\right)\right], \tag{18}$$

where $\Delta\eta_{L,\mathrm{ref}}$ is the reference viscosity contrast as calculated from equation (12), $\Delta\eta$ is the viscosity contrast introduced by mantle dehydration, h_{ref} is the thickness of reference thermal boundary layer expected in the absence of dehydration stiffening ($\equiv D/Nu_{\mathrm{ref}}$). Note that the depth extent of dehydration stiffening is not very sensitive to the wet solidus (which is affected by the mantle hydration state) but is instead well captured by the dry mantle solidus [*Hirth and Kohlstedt*, 1996], and this is why the formulation here is based on the dry solidus of mantle peridotite. With this definition of $\Delta\eta_L$, the effect of dehydration stiffening can be reflected properly both on the heat flow scaling (equation (9)) and on the criterion of plate tectonics (equation (15)). A few representative examples of heat flow scaling are given in Figure 2. With the effect of dehydration stiffening ($\Delta\eta > 1$), heat flow tends to be more suppressed for hotter mantle because thicker depleted lithosphere retards plate tectonics.

[12] The *Nu-Ra* relationship of equation (9) can be reduced to the following classical scaling for thermal convection [e.g., *Howard*, 1966]:

$$Nu \propto Ra^{1/3}, \tag{19}$$

if the lithospheric viscosity contrast $\Delta\eta_L$ is assumed to be constant. Equation (9) is thus more general, being able to

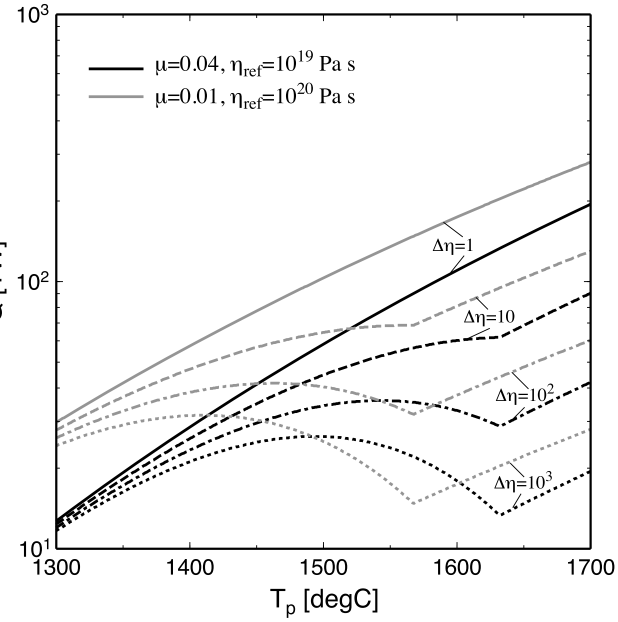

Figure 2. Examples of heat flow scaling based on equations (8)–(18). Activation energy E and reference temperature are set to 300 kJ mol^{-1} and 1350°C, respectively, for all cases. Solid curves are for the effective friction coefficient μ of 0.04 and the reference viscosity η_r of 10^{19} Pa s, and gray curves are for μ of 0.01 and η_r of 10^{20} Pa s. The effect of dehydration stiffening by mantle melting is greater for a higher viscosity contrast $\Delta\eta$ between depleted lithosphere and asthenosphere: $\Delta\eta$ = 1 (solid), 10 (dashed), 10^2 (dot-dashed), and 10^3 (dotted). Note that the effect of dehydration saturates at a high mantle temperature (~1600°C), resulting in a kink in predicted heat flow.

fully handle the effect of time-dependent mantle viscosity. Even though the above simple scaling has been repeatedly used in thermal evolution models [e.g., *Schubert et al.*, 1980; *McGovern and Schubert*, 1989; *Spohn and Breuer*, 1993], it is valid only for nearly isoviscous convection [*Solomatov*, 1995], and the rheology of Earth's mantle is anything but isoviscous. Note that the new scaling of equation (9), when combined with the effect of mantle melting (equation (18)), validates the earlier approximate solution based on the boundary layer theory [*Korenaga*, 2003, 2006]. The earlier approximate scaling has been criticized because it assumes a constant bending curvature for subducting plates [e.g., *Davies*, 2009]; the scaling of bending dissipation, which plays an important role in the boundary layer theory, is generally considered to be very sensitive to the bending curvature [*Conrad and Hager*, 1999a; *Buffett*, 2006], and present-day subducting slabs exhibit a wide range of bending curvature [*Lallemand et al.*, 2005]. A recent study on the scaling of bending dissipation, however, has revealed that the scaling is only weakly sensitive to the bending curvature if realistic mantle viscosity is considered [*Rose and Korenaga*, 2011; see also *Buffett and Heuret*, 2011]), undermining the criticism to the earlier scaling. Also note that equation (9) by itself does not tell us whether the present-day rate of bending dissipation is high or low. If the effective lithospheric viscosity contrast ($\Delta\eta_L$) is small, the rate of bending dissipation is low, and vice versa. As this viscosity contrast is a function of the effective friction coefficient and temperature-dependent viscosity, one can easily adjust the contribution of bending dissipation by changing, for example, the effective friction coefficient [*Rose and Korenaga*, 2011, Figure 13a]. What is important is the temporal trend of the contribution of bending dissipation, i.e., whether or not the contribution of bending dissipation was greater in the past. This question cannot be answered by looking at present-day plate tectonics, and this is where the scaling of equation (9) becomes useful. As seen in Figure 2, heat flow scaling with dehydration stiffening ($\Delta\eta > 1$) deviates more from the classical scaling at higher temperatures, indicating greater bending dissipation when the mantle was hotter in the past.

[13] The present-day mantle heat flux is the total terrestrial heat flux, 46 ± 3 TW [*Jaupart et al.*, 2007], minus the continental heat production, i.e.,

$$Q(0) = 46 - H_{cc}(0) + 3\varepsilon_3[\mathrm{TW}], \tag{20}$$

where ε_3 is another random variable with zero mean and unit standard deviation. For any given set of E, μ, and $\Delta\eta$, the reference viscosity η_r is chosen so that the predicted heat flux at the present-day, $Q(T_p(0))$, matches $Q(0)$ calculated from equation (20).

[14] Finally, it is convenient to define the convective Urey ratio [*Korenaga*, 2008b], which measures the relative importance of mantle heat production over mantle heat flux as

$$Ur(t) = H(t)/Q(t). \tag{21}$$

Both the numerator and the denominator are influenced by the uncertainty in the heat production of continental crust (equations (2) and (20)), so care must be taken when deriving the uncertainty of the Urey ratio. The present-day Urey ratio is estimated to be 0.23 ± 0.15 [*Korenaga*, 2008b]. Note that the present-day heat flux may be at the minimum of ~100 Myr-scale temporal variation and that the time-average heat flux, which is more appropriate to use in thermal evolution modeling, is likely to be somewhat higher than indicated in equation (20) [*Korenaga*, 2007a; *Loyd et al.*, 2007; *Becker et al.*, 2009]. This possibility would lower the present-day Urey ratio, though the precise extent of reduction is difficult to quantify because of uncertainties in the estimates of past heat flux.

2.4. Plate Velocity, Ocean Volume, and Mantle Water Content

[15] If the mantle is a closed system and its water content does not change with time, the above formulation would be sufficient to calculate a thermal history. Though it is still poorly quantified, however, subducting slabs could potentially bring surface water deep into the mantle [e.g., *Ito et al.*, 1983; *Jarrard*, 2003; *Smyth and Jacobsen*, 2006], and with some simplifying assumptions, it is possible to incorporate the effect of the net water flux into thermal evolution modeling. The key notion here is the constant freeboard [*Wise*, 1974], i.e., the mean sea level has always been close to the mean continental level. The constant freeboard is well supported by frequent inundations throughout the Phanerozoic,

and it is thought to be approximately valid in the Proterozoic as well [*Eriksson et al.*, 2006]. Even without eustasy, it is possible to inundate a continent by dynamic topography due to subducting slab [e.g., *Mitrovica et al.*, 1989; *Gurnis*, 1993], but global sea level changes still play a dominant role in the simultaneous inundation of multiple continents [*Harrison*, 1990; *Algeo and Seslavinsky*, 1995]. The abundant occurrence of submarine flood basalt magmatism in the Archean also suggests that the mean sea level had been sufficiently high to inundate most of continents.

[16] One robust constraint from these geological observations is that there has always been enough surface water to fill up the ocean basins at least to the mean continental level [*Korenaga*, 2008c]. As the capacity of global ocean basins is controlled by the speed of plate motion (or equivalently, the surface heat flux) [*Parsons*, 1982], the minimum ocean volume may be calculated together with a thermal history, and temporal variations in the ocean volume can then be used to provide a lower bound on the net water flux into the mantle. The non-zero net influx would of course modify the water content of the mantle and its viscosity, influencing the vigor of mantle convection. When a mantle can exchange water with oceans, therefore, care must be taken so that a thermal history is reconstructed in a self-consistent manner. One possible implementation is given in the following.

[17] First, average plate velocity is calculated from mantle heat flux as

$$v(t) = v(0)\left(\frac{Q(t)}{Q(0)}\frac{T_p(0)}{T_p(t)}\right)^2, \tag{22}$$

with the present-day velocity of 4 cm yr^{-1}. This is based on a scaling relation between surface heat flux and plate velocity, $Q \propto T_p\sqrt{v}$ [*Turcotte and Schubert*, 1982], which holds irrespective of heat flow scaling. In the above equation, the (average) aspect ratio of convection cells is implicitly assumed to be nearly constant through time. The aspect ratios of individual convection cells are clearly time-dependent as seen in the opening of the Atlantic ocean with the breakup of the supercontinent Pangea. What is important here is, however, the global average of individual aspect ratios. Some authors suggested that convection cells in the hot Archean mantle might be in general much smaller than present [*Hargraves*, 1986; *Abbott and Menke*, 1990], but as pointed out by *Korenaga* [2006], their arguments are based on the assumption of higher heat flux in the past, and if one considers the subductability of oceanic plates, the average aspect ratio of convection cells in the past should not be very different from the present.

[18] From plate velocity, the maximum age of seafloor can be calculated as

$$\tau_{\max}(t) = \tau_{\max}(0)\frac{v(0)}{v(t)}\sqrt{\frac{1-0.4F_{cc}(t)}{0.6}}, \tag{23}$$

with $\tau_{\max}(0) = 180$ Ma. This formulation takes into account that the present-day continental crust occupies 40% of Earth's surface and assumes that the average thickness of continental crust has been relatively constant [*Durrheim and Mooney*, 1991; *Galer and Mezger*, 1998]; a smaller continental mass in the past simply corresponds to wider ocean basins. The total ocean volume is then calculated as

$$V_o(t) = \int_0^{\tau_{\max}} \frac{dA_o}{d\tau}(\tau,t)d(\tau,t)d\tau, \tag{24}$$

where the area-age distribution of seafloor is given by

$$\frac{dA_o}{d\tau}(\tau,t) = \frac{2A(1-0.4F_{cc}(t))}{\tau_{\max}(t)}\left(1-\frac{\tau}{\tau_{\max}(t)}\right), \tag{25}$$

and the depth-age relation of seafloor is given by

$$d(\tau,t) = d_0(t) + b(t)\sqrt{\tau}, \tag{26}$$

in which d_0 is the zero-age depth (average depth to mid-ocean ridge axis) and b is the subsidence rate due to half-space cooling. At present, $d_0(0) = 2654$ m and $b(0) = 323$ m Ma$^{-1/2}$ [*Korenaga and Korenaga*, 2008], and the subsidence rate in the past depends on the internal temperature as [e.g., *Turcotte and Schubert*, 1982]

$$b(t) = b(0)\frac{T_p(t)}{T_p(0)}, \tag{27}$$

i.e., the seafloor subsides faster for a hotter mantle. The study of seafloor subsidence has a long history [e.g., *Parsons and Sclater*, 1977; *Stein and Stein*, 1992; *Carlson and Johnson*, 1994; *Smith and Sandwell*, 1997], but the above subsidence parameters correspond to the evolution of the 'normal' oceanic lithosphere, as delineated by *Korenaga and Korenaga* [2008]. The area-age distribution of equation (25) is the so-called triangular distribution, which is a good approximation to the present-day situation and arises naturally from subduction irrespective of seafloor age [*Parsons*, 1982]. The zero-age depth of seafloor d_o can be time-dependent, as it is controlled by the relative buoyancy of continental and oceanic regions on a global scale, and the following two end-member cases are considered: (1) in the case of closed-system evolution (constant ocean volume), it changes to satisfy the constant freeboard, or (2) in the case of open-system evolution (variable ocean volume), it stays constant with the present-day value. Note that the ocean volume calculation itself is not sensitive to the assumption of the constant aspect ratio of convection cells. If the aspect ratio is smaller, plate velocity becomes correspondingly smaller to satisfy the given heat flux, so the maximum age of seafloor is unaffected.

[19] In the case of open-system evolution, the amount of water stored in the mantle, V_{mw}, varies with time to compensate concurrent changes in the ocean volume and the continental mass:

$$V_{mw}(t) = V_{mw}(0) - [V_o(t) - V_o(0)] + [1 - F_{cc}(t)]V_{cw}(0), \tag{28}$$

where $V_{cw}(0)$ is the amount of water stored in the present-day continental crust ($V_{cw}(0)/V_o(0) = 0.18$) [*Wedepohl*, 1995]. The mantle water content cannot become negative, so when V_{mw} reaches zero, the ocean volume cannot increase any further, and the zero-age depth of seafloor starts to vary to satisfy the constant freeboard even in the case of open-system evolution. The variable hydration state of the mantle

Table 2. Summary of Successful Model Parameters: Case of Closed-System Evolution

Parameter	Mean	1σ	Correlation Coefficients $Ur(0)$	$Q(0)$	$H_{cc}(0)$	f_{mix}	μ	E	$\log_{10}\Delta\eta$
$Ur(0)$ [TW]	0.23	0.05	1.000	0.181	−0.489	0.078	−0.005	0.057	−0.550
$Q(0)$ [TW]	38.0	2.2	0.181	1.000	−0.630	0.005	−0.022	−0.085	−0.141
$H_{cc}(0)$ [TW]	7.6	1.4	−0.489	−0.630	1.000	−0.040	0.007	0.041	0.283
f_{mix}	0.48	0.29	0.078	0.005	−0.040	1.000	0.014	−0.040	0.078
μ	0.027	0.011	−0.005	−0.022	0.007	0.014	1.000	−0.134	0.119
E [kJ/mol]	260	46	0.057	−0.085	0.041	−0.040	−0.134	1.000	0.323
$\log_{10}\Delta\eta$	2.6	0.2	−0.550	−0.141	0.283	0.078	0.119	0.323	1.000

may be reflected in its rheology as [*Fraeman and Korenaga*, 2010]

$$\eta_r(t) = \eta_r(0)\exp\left[\left(1 - \frac{V_{mw}(t)}{V_{mw}(0)}\right)\log(\Delta\eta(0))\right], \qquad (29)$$

and

$$\Delta\eta(t) = \exp\left[\left(\frac{V_{mw}(t)}{V_{mw}(0)}\right)\log(\Delta\eta(0))\right]. \qquad (30)$$

When the mantle becomes completely dry ($V_{mw}(t) = 0$), for example, no viscosity contrast would be introduced by mantle melting ($\Delta\eta(t) = 1$) because the effect of dehydration stiffening is already taken up by the entire mantle through the reference viscosity ($\eta_r(t) = \eta_r(0)\Delta\eta(0)$).

2.5. Monte Carlo Sampling

[20] The above theoretical formulation involves a number of parameters, and besides planetary constants such as the mantle depth, most of input parameters are not precisely known. It is therefore important to understand what part of modeling results are robust (i.e., insensitive to such uncertainty in input data) by fully exploring the permissible parameter space. Eight parameters are identified to this end, including three random variables for the thermal budget ε_i ($i = 1 - 3$), one random variable for continental growth f_{mix}, the activation energy of temperature-dependent viscosity E, the effective friction coefficient μ, the viscosity contrast due to dehydration $\Delta\eta$, and the amount of water in the present-day mantle $V_{mw}(0)$. These parameters are sampled from the following ranges with equal probability (i.e., uniform distribution): $\varepsilon_i = [-1, 1]$, $f_{mix} = [0, 1]$, $E = [200, 400]$ (kJ mol^{-1}) [*Korenaga*, 2006; *Korenaga and Karato*, 2008], $\mu = [0.01, 0.05]$, $\log_{10}\Delta\eta = [1, 3]$ [*Faul and Jackson*, 2007; *Korenaga and Karato*, 2008], and $V_{mw}(0)/V_o(0) = [0.2, 1]$. The range of μ corresponds to effective friction coefficients with high pore fluid pressures [*Korenaga*, 2007b]. The range of the mantle water content is based on the water content of the source mantle for mid-ocean-ridge basalts (142 ± 85 ppm) [*Saal et al.*, 2002]. The majority of the mantle is likely to be represented by this type of mantle (MORB-source mantle) [*Lyubetskaya and Korenaga*, 2007b; *Korenaga*, 2009]. Though the storage capacity of the mantle transition zone is very high [*Hirschmann*, 2006] and some regions exhibit notable electrical conductivity [e.g., *Kelbert et al.*, 2009; *Khan et al.*, 2011], the petrology of mid-ocean ridge basalts and ocean island basalts indicates that the transition zone is unlikely to be globally much more hydrous than the upper mantle [e.g., *Hirschmann et al.*, 2005; *Hauri et al.*, 2006]. Imagine, for example, a parcel of mantle materials rising from the lower mantle toward a mid-ocean ridge. Such parcel is unlikely to have melted when passing through the transition zone [*Hauri et al.*, 2006], so its water content does not change during its ascent. The water content of the MORB-source mantle is quite low (i.e., 0.01–0.02 wt%), being well below the water capacity of the mantle possibly at all depths [e.g., *Inoue et al.*, 2010]. The water concentration in the upper mantle is thus expected to reflect a mantle-wide average, probably similar to a situation envisioned by *Richard et al.* [2002]. Note that with this (low) level of water concentration, water partitioning among olivine high-pressure polymorphs is not relevant to actual water distribution within the convecting mantle. Equilibrium partitioning among different mantle layers, as often envisioned by mineral physicists [e.g., *Inoue et al.*, 2010], is only achievable in a static mantle with an extremely long timescale (i.e., chemical diffusion timescale for the whole mantle, which is much longer than the age of the universe).

[21] For each combination of randomly sampled variables, equation (1) is integrated back to 4.6 Ga ago, and the success of each model run is judged on the basis of a predicted thermal history $T_p(t)$. The deviation from the petrological estimate [*Herzberg et al.*, 2010] is measured by the following cost functional,

$$\chi^2(T_p) = \int_0^{t_1}\left(\frac{T_p(t) - T_p^{\mathrm{ref}}(t)}{\sigma_T}\right)^2 dt \Big/ \int_0^{t_1} dt, \qquad (31)$$

where $T_p^{\mathrm{ref}}(t) = 1580 - 25.6(t-3)^2$, $\sigma_T = 50$ K, and $t_1 = 3.5$ Ga. Only modeling results with $\chi^2 < 1$ are retained for further consideration.

3. Results

[22] Obtaining successful solutions by Monte Carlo sampling was more efficient for the case of closed-system evolution than that of open-system evolution; about one out of ten trials satisfied the condition of $\chi^2 < 1$ for the former, and the success rate was around five times less for the latter. For both cases, I conducted ten sampling runs starting with different seeds, and each run was continued until 10^4 successful solutions were collected. For each sampling run, the mean values of successful model parameters and their standard deviations were calculated along with correlation coefficients between different parameters (Tables 2 and 3). These statistics vary little among the ten sampling runs; mean values and their standard deviations do not vary more than ±1% and ±3%, respectively, and correlation coefficients are consistent

Table 3. Summary of Successful Model Parameters: Case of Open-System Evolution

Parameter	Mean	1σ	Correlation Coefficients							
			$Ur(0)$	$Q(0)$	$H_{cc}(0)$	f_{mix}	μ	E	$\log_{10}\Delta\eta$	$V_{mw}(0)/V_o(0)$
$Ur(0)$ [TW]	0.28	0.04	1.000	0.294	−0.619	0.020	0.035	0.148	−0.199	−0.088
$Q(0)$ [TW]	37.9	2.0	0.294	1.000	−0.694	0.042	−0.009	−0.143	−0.032	0.052
$H_{cc}(0)$ [TW]	7.1	1.4	−0.619	−0.694	1.000	−0.057	−0.012	0.019	0.110	0.025
f_{mix}	0.51	0.29	0.020	0.042	−0.057	1.000	−0.011	−0.056	−0.002	−0.028
μ	0.027	0.012	0.035	−0.009	−0.012	−0.011	1.000	−0.221	0.119	0.017
E [kJ/mol]	252	39	0.148	−0.143	0.019	−0.056	−0.221	1.000	0.239	0.078
$\log_{10}\Delta\eta$	2.7	0.2	−0.199	−0.032	0.110	−0.002	0.119	0.239	1.000	0.088
$V_{mw}(0)/V_o(0)$	0.76	0.18	−0.088	0.052	0.025	−0.028	0.017	0.078	0.088	1.000

within ±0.04. Results shown in this section are thus based on the statistics of one sampling run (i.e., 10^4 successful solutions).

3.1. Closed-System Evolution

[23] The case of closed-system evolution assumes no interaction between the convecting mantle and the oceans; there is no net water flux into or out of the mantle, so the mantle water content is constant over time. With thicker dehydrated lithosphere suppressing the convective vigor of a hotter mantle, reproducing a thermal history consistent with the petrological constraints (Figure 3a) is possible for a range of model parameters (Figures 4 and 5). In particular, the effect of continental growth on thermal evolution is of

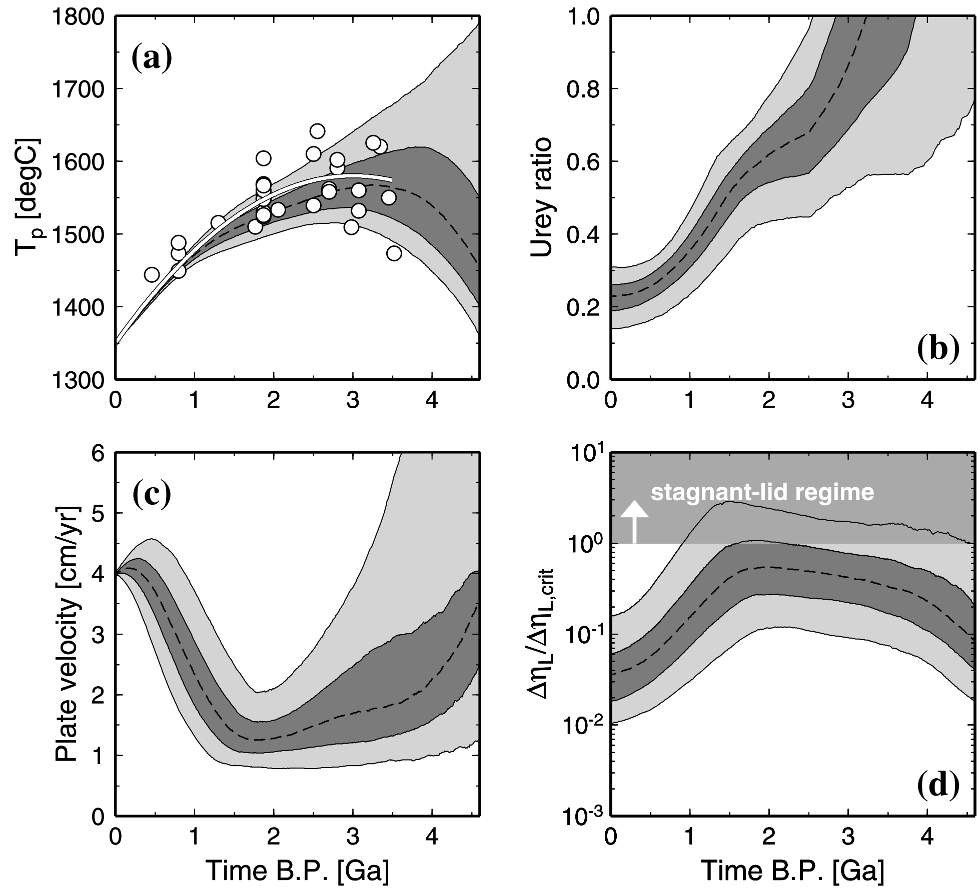

Figure 3. Results of thermal evolution modeling are shown as a function of time, for the case of closed-system evolution. Dashed curves correspond to the median of 10^4 successful solutions. Dark gray regions cover from the first to the third quartile, representing the 50% of total solutions, whereas light gray regions cover from the 5th to 95th percentile. Quantiles such as quartile and percentile are used instead of standard deviations because the distributions of some variables are notably different from Gaussian. (a) Mantle potential temperature. Open circles denote petrological estimates on the paleotemperature of the convecting mantle [*Herzberg et al.*, 2010], and a thick white curve denotes $T_p^{ref}(t) = 1580 - 25.6(t-3)^2$, which is used in equation (31). (b) Convective Urey ratio. (c) Average plate velocity. (d) Lithospheric viscosity contrast normalized by the threshold for the transition to stagnant-lid convection (equation (15)).

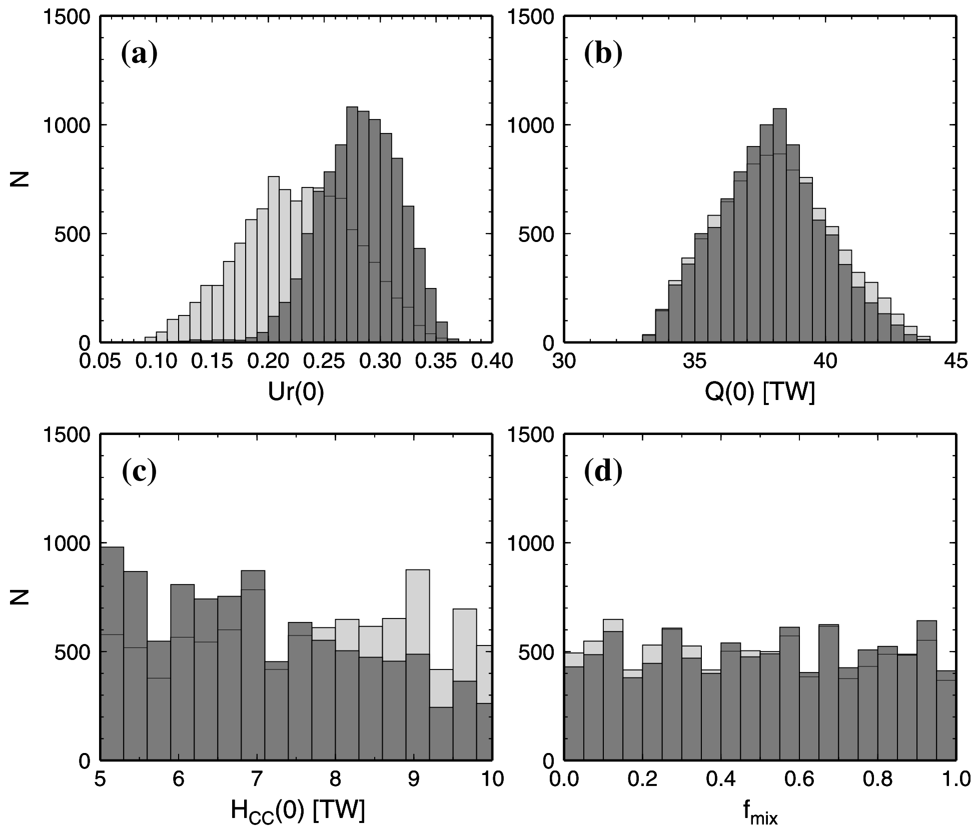

Figure 4. The a posteriori distributions of model parameters based on 10^4 successful runs. Light-shaded histograms are for closed-system evolution and dark-shaded ones for open-system evolution. (a) Present-day Urey ratio $Ur(0)$. (b) Present-day mantle heat flux $Q(0)$. (c) Present-day continental heat production $H_{cc}(0)$. (d) Mixing parameter for continental growth f_{mix}.

minor significance as indicated by the relatively uniform distributions of $H_{cc}(0)$ and f_{mix}. In contrast, it is easier to find a successful solution with a lower activation energy (Figure 5b) and a higher viscosity contrast between dry and wet mantle (Figure 5c) because both help to suppress the vigor of convection of a hotter mantle (equation (9)). Note that the success of thermal history reconstruction may not seem to depend on the effective friction coefficient (Figure 5a), but this is because, as described in section 2.3, the reference viscosity becomes lower for a higher friction coefficient so that the predicted mantle heat flux at present always matches the observational constraint (Figure 6). Too high friction coefficient can be precluded because it would correspond to an unrealistically low reference viscosity [cf. *Korenaga*, 2010a, p. 14].

[24] Results described so far are nothing really new. The possibility that more sluggish plate tectonics in the past can satisfy both the present-day thermal budget and the rate of secular cooling has been suggested by *Korenaga* [2003] based on the boundary layer theory. What is presented here is a confirmation of this idea by using a heat flow scaling law built on fully dynamic simulations and a demonstration of its robustness by extensively exploring the parameter space.

[25] This seemingly successful case of closed-system evolution, however, has one serious drawback; the effective lithospheric viscosity contrast approaches the critical value for ~1.5–3 Ga ago (Figure 3d). When the mantle was hotter in the past, its internal viscosity is lower due to its temperature dependency, and so is the convective stress. At the same time, dehydrated lithosphere is thicker, so it becomes more difficult for convective stress to break the stiff lithosphere and initiate subduction. Though ~75% of model runs remain in the mode of plate tectonics, the overall trend of approaching the threshold in the last 1.5 Ga is unsettling because the criterion (equation (15)) is not exact; plate tectonics would be guaranteed only when $\Delta\eta_L/\Delta\eta_{L,crit}$ is sufficiently smaller than unity [*Korenaga*, 2010a]. The possibility of intermittent plate tectonics, i.e., alternating stagnant-lid convection and plate tectonics, has been suggested [e.g., *O'Neill et al.*, 2007; *Silver and Behn*, 2008], but this idea is in conflict with the continuous operation of plate tectonics during the Proterozoic as suggested by the history of passive margins [*Bradley*, 2008], and it would also result in an undulating thermal history [*Silver and Behn*, 2008; *Korenaga*, 2008a] that is inconsistent with petrological data [*Herzberg et al.*, 2010].

[26] Note that more sluggish plate tectonics in the past means older seafloor on average and thus greater seafloor subsidence, so in the closed-system evolution with a constant ocean volume, the zero-age depth of seafloor must rise rather substantially (at the rate of ~1 km Ga^{-1}) to satisfy the constant freeboard, and mid-ocean ridges may have been subaerial before ~1.5 Ga ago (Figure 7a). If such shallowing does not take place and the ridge depth stays constant, the

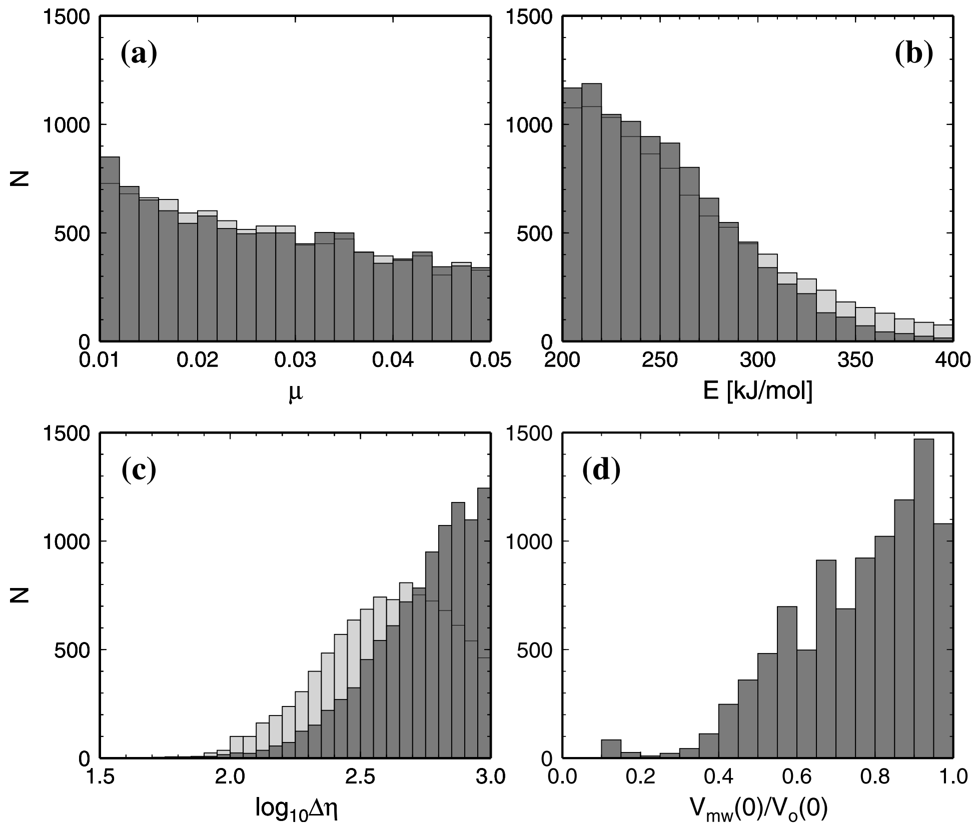

Figure 5. Same as Figure 4 but for (a) effective friction coefficient μ, (b) activation energy for mantle viscosity E, (c) viscosity contrast caused by dehydration stiffening $\Delta\eta$, and (d) the amount of water in the present-day mantle $V_{mw}(0)$ normalized by the present-day ocean volume $V_o(0)$.

ocean volume in the past has to be greater to satisfy the constant freeboard (Figure 7b). A time-varying ocean volume is possible only for the open-system evolution, which is explored in the next section.

3.2. Open-System Evolution

[27] The bulk silicate Earth (the mantle and the crust) is estimated to contain approximately one ocean worth of water at present (section 2.5), so more voluminous oceans could potentially be explained by a drier mantle in the past. The reconstructed thermal history with water exchange between the mantle and the surface is similar to that in the case of closed-system evolution, though it tends to have higher mantle temperature in the Archean (Figure 8a). The distributions of successful model parameters are mostly similar to those for the closed-system evolution (Figures 4 and 5); a notable exception is the present-day Urey ratio, which is clustered around a slightly higher value, ~0.28 (Figure 4a).

[28] The zero-age seafloor can stay at the present-day depth back to ~3–4 Ga ago (Figure 9a) because the ocean volume is greater in the past to meet the constant freeboard (Figure 9b). The water content of the mantle in the past is correspondingly lower, and the mantle is likely to have been entirely dry in the Hadean. The hydration of the mantle could have started in the Hadean or as late as in the late Archean (Figure 9b). More gradual continental growth (i.e., $f_{\mathrm{mix}} \ll 1$, equation (7)) and a lower water amount of the

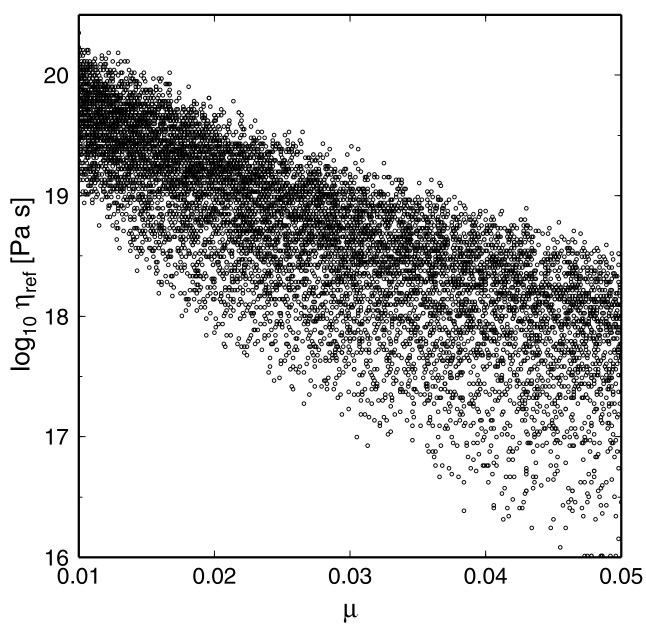

Figure 6. Covariation of the effective friction coefficient and the reference viscosity for the case of closed-system evolution. The case of open-system evolution exhibits similar correlation.

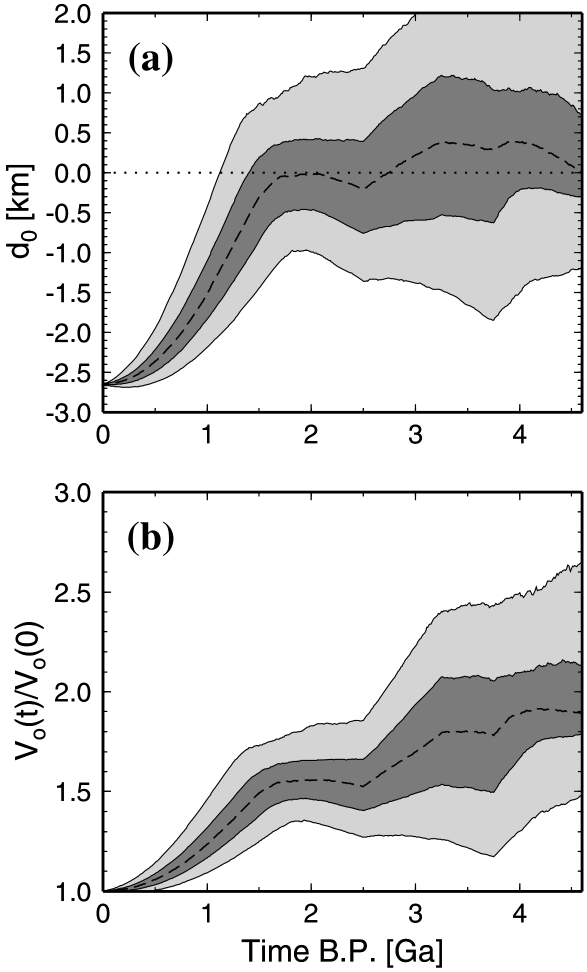

Figure 7. Same as Figure 3 but for (a) the depth of zero-age seafloor, d_0 and (b) hypothetical ocean volume V_o in case of time-invariant zero-age seafloor depth.

present-day mantle (Figure 5) favor the late onset of mantle hydration. The drier mantle in the past reduces the effect of dehydration stiffening on mantle dynamics (e.g., no effect is expected for the melting of an entirely dry mantle), so surface heat flow and plate velocity in the past are not suppressed as much as in the closed-system evolution. This is why the predicted thermal history tends to be hotter and the present-day Urey ratio needs to be higher in the open-system evolution. For the same reason, variations in the ocean volume are not as much as predicted from the closed-system evolution (Figure 7b). Also, reduction in plate velocity for the last 1 Ga is only ~25% (Figure 8c), which is actually more consistent with the geological estimate based on the life span of passive margins [*Bradley*, 2008].

[29] The most important aspect of the open-system evolution is that the likelihood of plate tectonics is nearly constant throughout the Earth history ($\Delta\eta_L/\Delta\eta_{L,crit} \sim 0.1$, Figure 8d). The drier mantle in the past helps to maintain large enough convective stress, or equivalently, reduce the effect of dehydration stiffening. This serves as a posteriori justification of plate tectonics assumed for the reconstructed thermal history (Figure 8a). In other words, the open-system evolution considered here can be regarded as fully internally consistent; the same cannot be said for the case of closed-system evolution. This internal consistency has important implications for the nature of ocean-mantle interaction as discussed later (section 4.2).

4. Discussion and Outlook

4.1. Heat Flow Scaling and Thermal Budget

[30] The heat flow scaling law of equation (9) depends on the assumed mantle rheology (η_r, E, μ, and $\Delta\eta$ when the effect of mantle melting is considered) (Figure 2), which varies among different runs. The ensemble of successful runs, however, exhibits a well-defined trend (Figure 10); heat flow and mantle temperature are strongly negatively correlated up to ~1500°C in the closed-system evolution, whereas heat flow is relatively constant up to ~1600°C in the open-system evolution. When the mantle is sufficiently hot (e.g., >1600°C in the open-system evolution), heat flow is higher for a hotter mantle, but for the temperature range relevant to the last 3 Ga or so (Figure 3a), such conventional scaling clearly does not apply. The pronounced inverse relation between mantle temperature and heat flux in Figure 10a is owning to the thicker dehydrated lithosphere for hotter mantle, but as indicated by Figure 3d, simply having thicker lithosphere would jeopardize the operation of plate tectonics in the Proterozoic, so this heat flow scaling, which is based on the assumption of plate tectonics, is on the verge of self-consistency. Gradual mantle hydration over the Earth history, as in the case of open-system evolution, alleviates the situation by reducing the viscosity contrast between the convecting mantle and the lithosphere, and at the same time, heat flow becomes virtually insensitive to mantle temperature. It is interesting that this deceptively simple scaling results from combining realistic complications in mantle dynamics, i.e., chemical differentiation and ocean-mantle interaction.

[31] Note that there may be other ways to achieve this relatively constant heat flux over a range of mantle temperature, though there are few proposals with a concrete physical mechanism. It is possible, for example, to create a temperature-insensitive scaling by assuming that plate thickness stays constant regardless of mantle temperature [*Conrad and Hager*, 1999b; *Labrosse and Jaupart*, 2007], but the validity of this assumption is rarely discussed. One can quantify the maximum plate thickness based on the stability of thermal boundary layer, and without taking account the effect of dehydration stiffening, plates should become thinner for a hotter mantle [*Korenaga*, 2003]. It is also difficult to maintain plate tectonics with constant plate thickness and a hotter mantle unless the temperature-dependent viscosity of the mantle is somehow compensated, e.g., by gradual hydration as considered in this study. In this regard, the mantle dynamics dominated by grain growth [*Solomatov*, 2001] is so far the only other mechanism that could potentially yield a constant heat flux scaling. In this hypothesis, a hotter mantle does not necessarily be less viscous if the bulk behavior of the mantle is dominated by diffusion creep, which is very sensitive to grain size. A hotter mantle may have larger grains on average because grains grow faster at higher temperatures, and diffusion creep is slower for larger grains. If the grain size evolution over the Earth history is such that the average viscosity of the mantle stays relatively

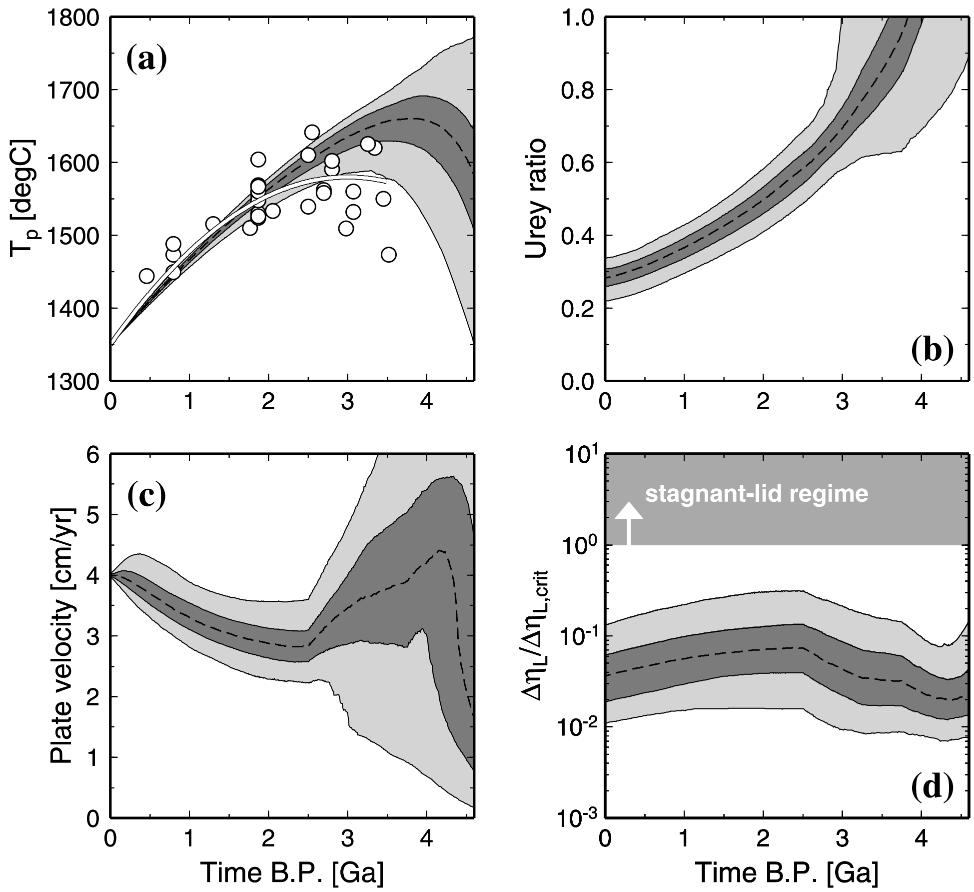

Figure 8. Same as Figure 3 but for the case of open-system evolution.

constant despite its secular cooling, the convective heat flux would become insensitive to the internal temperature.

[32] Regardless of how a constant heat flux is achieved, this scaling is essential to reconstruct a thermal history consistent with petrological and geochemical constraints, as illustrated in Figure 11. The present-day convective Urey ratio $Ur(0)$ is estimated to be 0.23 ± 0.15 [*Korenaga*, 2008b], and with a classical heat flow scaling (Figure 11a), we would have a divergent thermal history in the Proterozoic, known as thermal catastrophe [*Christensen*, 1985] (Figure 11b). It is possible to avoid the catastrophe by assuming a much higher Urey ratio (~0.7–0.8; [e.g., *Schubert et al.*, 1980, 2001]), though this solution does not conform to the chemical composition of Earth's mantle [*Hart and Zindler*, 1986; *McDonough and Sun*, 1995; *Lyubetskaya and Korenaga*, 2007a]. There are a variety of geochemical arguments for a hidden geochemical reservoir enriched in heat-producing elements [e.g., *Allegre et al.*, 1996; *Hofmann*, 1997; *Albarede and van der Hilst*, 2002; *Porcelli and Turekian*, 2004], but it is important to understand that these arguments arise from global mass balance and are thus consistent with the low Urey ratio (i.e., 0.23 ± 0.15). These arguments simply tell us that the part of the mantle sampled by mid-ocean ridge magmatism appears to be too depleted in a certain group of trace elements (including heat-producing elements) to match the difference between the composition of the primitive mantle and that of continental crust. In other words, if we use mantle composition models based on mid-ocean ridge samples [e.g., *Jochum et al.*, 1983; *Salters and Stracke*, 2004; *Workman and Hart*, 2005], the convective Urey ratio would be even lower than 0.2, and an enriched hidden reservoir has been proposed to bring the Urey ratio up to the value expected from the theoretical composition of the primitive mantle (equivalent to the bulk silicate Earth). Because estimating the mantle composition from mid-ocean ridge samples could suffer from various sources of uncertainty, however, the mass of a hidden reservoir does not have to be substantial as previously thought and could be trivially small [e.g., *Lyubetskaya and Korenaga*, 2007b; *Korenaga*, 2008b]. Also note that, whereas seismological observations point to chemical heterogeneity in the deep mantle [e.g., *Masters et al.*, 2000], often referred to as "chemical piles," these observations do not constrain the trace element budget of such chemical piles. It is possible that chemical piles are enriched in iron but not in heat-producing elements. Such situation may be achieved, for example, if chemical piles represent subducted oceanic crust, because subduction processes could alter the trace element composition of oceanic crust rather substantially [e.g., *Kelemen et al.*, 2004].

[33] Moreover, a high-Urey-ratio solution predicts a thermal history to be concave upward (Figure 11b); the rate of secular cooling in the Phanerozoic and the Proterozoic is lower than that in the Archean, which is actually opposite to what is suggested by petrological data [*Herzberg et al.*, 2010]. To reproduce the observed trend of secular cooling, the convective heat flux must cross the internal heat

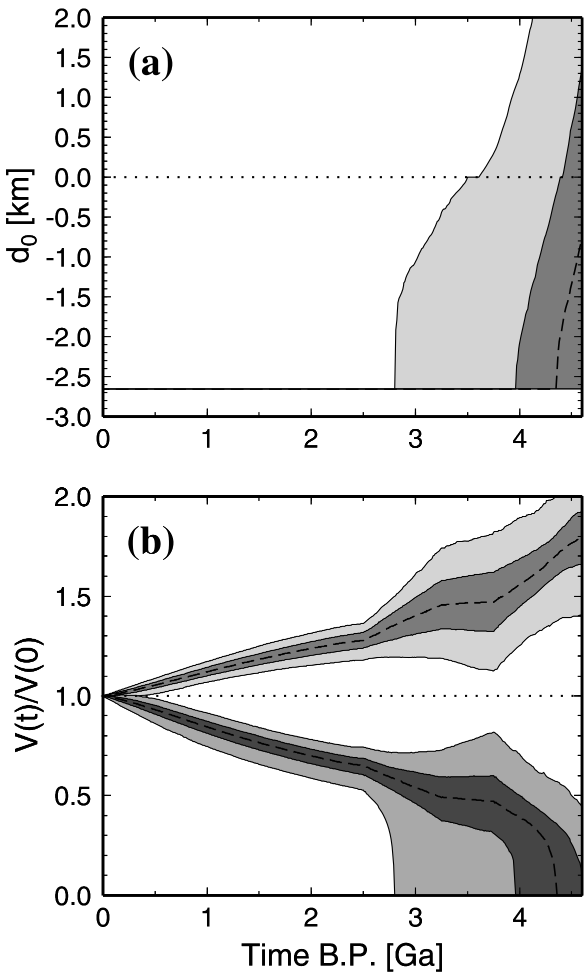

Figure 9. (a) Same as Figure 7 but for the case of open-system evolution. (b) Both ocean volume $V_o(t)$ (lighter gray shades) and mantle water $V_{mw}(t)$ (darker gray shades) are shown after normalized by their present-day values.

production sometime in the Archean, which is only possible with a (nearly) time-invariant heat flux. The present-day Urey ratio must not be substantially higher than ~0.3, because the crossover of heat flux and heat production would then take place too recently (Figure 11d), resulting in too cold a thermal history (Figure 11b). Thus, the concave-downward thermal history as indicated by petrology requires both temperature-insensitive heat flux and a low Urey ratio. To quantify the robustness of this concave-downward nature, bootstrap resampling [*Efron*, 1982] was applied to the data of *Herzberg et al.* [2010] as follows. Each of resampled ensemble is fitted with the following parabola:

$$T_p(t) = at^2 + bt + 1350, \tag{32}$$

which passes through the present-day condition, and the statistics based on 10^3 bootstrap ensembles is found to be: $a = -30.44 \pm 4.68$ and $b = 165.77 \pm 10.90$, where uncertainty corresponds to one standard deviation. The negativity of the parameter a, which is equivalent to being concave downward, is thus indisputable.

[34] To explore the possibility that a high-Urey-ratio solution could resemble the concave downward thermal history, Monte Carlo sampling of the closed system evolution is repeated with the classical heat flow scaling of equation (19). That is, the viscosity contrast $\Delta\eta_L$ in equation (9) is set to unity. To allow high Urey ratios, the a priori range on the random variable ε_1 in equation (2) is modified from [−1, 1] to [−1, 8]. Finding a solution with $\chi^2 < 1$ is found to be difficult, and the criterion is relaxed to $\chi^2 < 1.5$. The a posteriori distribution of such solutions is shown in Figure 12. As already discussed, the concave upward nature of high-Urey-ratio solutions makes it difficult to fit the petrological data (Figure 12a), which explains why it is difficult to satisfy $\chi^2 < 1$. The convective Urey ratio is

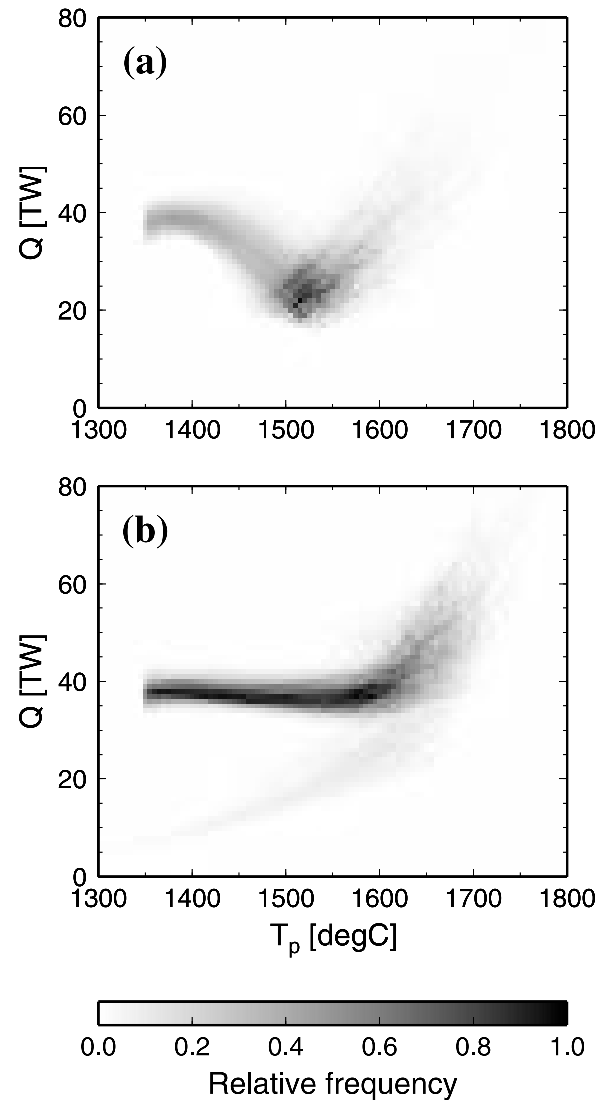

Figure 10. Relation between mantle potential temperature and convective heat flux based on 10^4 successful model runs for (a) closed-system evolution and (b) open-system evolution. In Figure 10b, some data points run from $Q \sim 10$ TW and $T_p \sim 1400$°C to higher Q and T_p, and they represent the evolution of an entirely dry mantle in the early Earth (Figure 9), i.e., corresponding to the case of $\Delta\eta = 1$ in Figure 2.

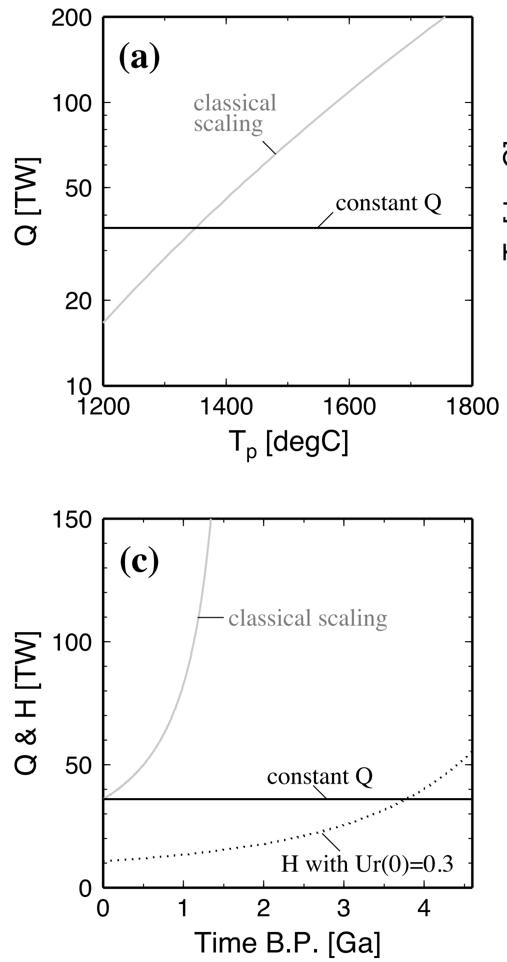

Figure 11. Consequences of different heat flow scaling and different heat production in predicted thermal history. (a) Temperature-insensitive heat flow scaling (solid), which is a good approximation to the one shown in Figure 10b, and classical scaling used in a number of previous studies on thermal evolution (see *Korenaga* [2008b] for review). (b) Thermal history prediction for four combinations of heat flow scaling and internal heat production. Constant heat flux with a low present-day Urey ratio (solid) is the only one that can produce a concave-downward thermal history with an average cooling rate of ~100 K Ga^{-1}. Classical scaling with a low Urey ratio results in thermal catastrophe (gray). Classical scaling with a high Urey ratio (gray dashed) can reproduce a reasonable cooling rate but a thermal history is concave upward. Constant heat flux with a high Urey ratio (dashed) results in too cold a thermal history. (c) Evolution of convective heat flux Q (solid for constant heat flux and gray for classical scaling) and internal heat production H (dotted) with a low present-day Urey ratio. (d) Same as Figure 11c but with a high present-day Urey ratio.

0.70 ± 0.02 at present, which stays relatively constant during the Proterozoic (Figure 12b). With lower Urey ratios, it would be possible to fit the high cooling rate during the Proterozoic, but such solutions would lead to thermal catastrophe and could not satisfy the low cooling rate during the Archean (Figure 11b). The activation energy E (not shown here) is clustered around the minimum (200 kJ mol^{-1}), barely exceeding 250 kJ mol^{-1}. This low activation energy reduces the temperature sensitivity of heat flow scaling, allowing the crossover of heat loss and heat production at ~4 Ga ago (i.e., Urey ratio greater than unity). One may wonder if a better fit may be achieved by starting thermal history calculation with a higher present-day temperature (e.g., 1400°C), but the calculation has to start with the present-day temperature of the MORB-source mantle, which is estimated to be 1350°C by *Herzberg et al.* [2007] using the same method used in *Herzberg et al.* [2010]. During the Proterozoic, predicted plate velocity increases rather drastically (Figure 12c), while the zero-age depth of seafloor does not vary much from the present-day value. This relative constancy of the zero-age depth indicates that, with classical scaling, the constant freeboard can be satisfied without changing the ocean volume, as previously shown by *Schubert and Reymer* [1985], so there is no need to explore the possibility of the open system evolution. Note that we cannot test the validity of plate tectonics assumption in this exercise because the effective lithospheric viscosity contrast is arbitrarily set to unity. To sum, high-Urey-ratio solutions do not satisfy the petrological constraints on the thermal history (Figure 12a), the geochemical constraints on the

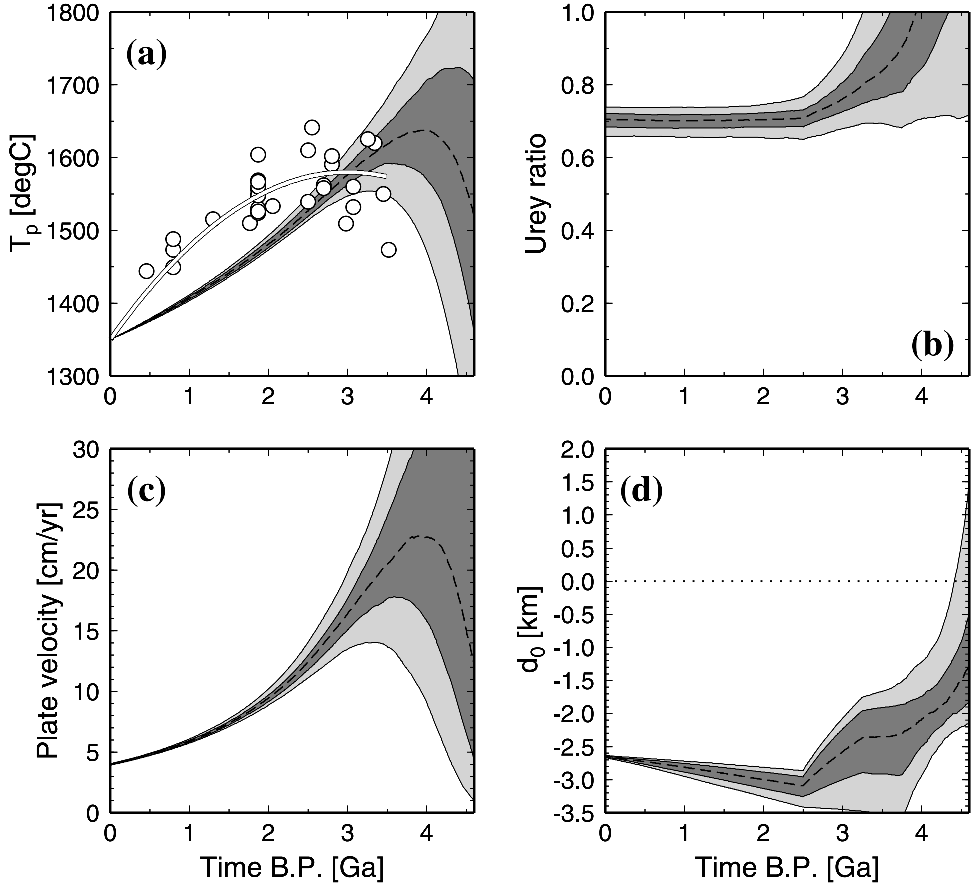

Figure 12. Results of thermal evolution modeling with classical heat flow scaling for the case of closed-system evolution. Legend is same as Figure 3. (a) Mantle potential temperature. (b) Convective Urey ratio. (c) Average plate velocity. (d) The depth of zero-age seafloor, d_0.

thermal budget (Figure 12b), and the geological constraints on the tempo of plate tectonics (Figure 12c).

4.2. Model Uncertainty and Nonuniqueness

[35] The thermal evolution modeling presented here has a somewhat complex theoretical formulation (section 2), including a heat flow scaling law that can handle pseudoplastic rheology, the effect of mantle melting, and water exchange between the mantle and the surface. Still, the modeling philosophy is the same as that of previous parameterized convection studies, i.e., to understand a gross behavior of planetary evolution on the basis of scaling laws that relate average mantle properties. This philosophy necessitates a variety of simplifications in theoretical formulation, and it is important to understand how modeling results may be affected by them. In this section, therefore, I discuss the following simplifications in some detail: (1) the assumption of whole mantle convection, (2) the use of pseudoplastic rheology in the heat flow scaling law, and (3) the relation between plate tectonics and the ocean volume.

[36] As the surface heat flux appearing in the global heat balance (equation (1)) is parameterized as a function of bulk mantle properties such as potential temperature (equation (10)) and water content (equation (29)), so whole mantle convection is implicitly assumed. The notion of layered-mantle convection, with a deep mantle reservoir sequestered from mantle circulation at shallower depths, has often been discussed in the literature [e.g., *Richter*, 1985; *Silver et al.*, 1988; *Hofmann*, 1997; *Tackley*, 2000; *Boyet and Carlson*, 2005], though the volumetric significance of such deep mantle reservoir is highly uncertain [*Korenaga*, 2008b]. Though this issue has long been overlooked in the past, it is important to recognize that the chemical composition models of Earth's mantle assume whole mantle convection [e.g., *McDonough and Sun*, 1995; *Palme and O'Neill*, 2004; *Lyubetskaya and Korenaga*, 2007a; *Korenaga*, 2009]; otherwise one cannot estimate the mantle composition (or equivalently, mantle heat production) in a self-consistent manner, and the thermal budget of Earth becomes undefined. Also, if the putative deep mantle reservoir were volumetrically significant and could play an important role in the thermal evolution of Earth, one has to specify how to parameterize the heat loss of the deep reservoir, which is expected to depend on the details of mantle rheology at the mid-mantle or lower-mantle condition, but our understanding of deep mantle rheology is still highly limited. Exploring the possibility of layered-mantle convection [e.g., *Spohn and Schubert*, 1982; *Honda*, 1995] is thus deemed better left for future studies. It is noted, however, the concave-downward thermal history as indicated by petrological data [*Herzberg et al.*, 2010] does not conform to the presence of a highly radioactive deep reservoir (section 4.1). Also, the possibility

of the high convective Urey ratio (0.7–0.8) assumed in conventional thermal evolution models [e.g., *Schubert et al.*, 1980; *Davies*, 2009] is only marginally consistent with geoneutrino observations [*Gando et al.*, 2011].

[37] The heat flow scaling law of equation (9) is parameterized with the internal Rayleigh number and the lithospheric viscosity contrast; the former is controlled by the ductile component of mantle rheology whereas the latter is by both ductile and brittle components. Though this parameterization with one internal parameter and one near-surface parameter is in a reasonably general form, the parameterization of the lithospheric viscosity contrast (equation (12)) depends critically on the assumption that the weakening of lithosphere can be represented by an effective friction coefficient. This assumption was first introduced by *Moresi and Solomatov* [1998] and is known to require a friction coefficient much lower than laboratory experiments indicate [e.g., *Byerlee*, 1978]. It has been common to justify such low friction coefficient by referring to the study of the San Andreas fault, which appears to be much weaker than a conventional friction coefficient suggests, but the study of this fault would only tell us the strength of continental crust and has no bearing on that of oceanic lithosphere, which is most relevant to the operation of plate tectonics. An effective friction coefficient can be reduced considerably if pore fluid exists and its pressure approaches lithostatic, but oceanic lithosphere is known to be dehydrated by mantle melting beneath mid-ocean ridges [*Hirth and Kohlstedt*, 1996; *Evans et al.*, 2005]. Without providing a physical mechanism that can rehydrate oceanic lithosphere, it is difficult to justify modeling plate-tectonic convection using a low effective friction coefficient. Thermal cracking can potentially be such a mechanism [*Korenaga*, 2007b] though its plausibility needs to be investigated further. One concern has been the limited penetration of thermal cracking, which can fracture oceanic lithosphere only down to the isotherm of ~700°C. In terms of bending deformation, however, fracturing down to the mid-lithospheric depth has been shown to be almost as effective as fracturing the entire lithosphere [*Rose and Korenaga*, 2011], so the thermal cracking hypothesis appears to be promising.

[38] Another issue regarding the assumed mantle rheology is the use of a single ductile deformation mechanism with a global reference viscosity (equations (11) and (29)). Reference viscosity (i.e., viscosity at the reference potential temperature) is likely to be depth-dependent [e.g., *Hager*, 1984; *King*, 1995], however, and there also exist a multitude of deformation mechanisms with different dependencies on temperature, pressure, and water content [e.g., *Karato and Wu*, 1993; *Hirth and Kohlstedt*, 2003]. The activation energy E and the reference viscosity η_r in this study should thus be regarded as effective parameters that aim to represent the net outcome of multiple deformation processes on a whole mantle scale. The range of activation energy explored here (200–400 kJ mol^{-1}) is, for example, based on the rheology of the upper mantle, and it may not be appropriate when calculating the internal Rayleigh number for the entire mantle. The role of lower mantle rheology in the global heat flow scaling is a subject that warrants careful consideration.

[39] The ocean volume in the past is calculated from the convective heat flux through several scaling relations (equations (22)–(27)). While these scaling relations themselves can readily be derived from physical or geometrical arguments, the entire procedure is based on the following two major assumptions: (1) the thickness of the continental crust has been constant, and (2) the zero-age depth of seafloor has also been constant in the case of open-system evolution. The thickness of continental crust may have been different in the past, and unlike the thickness of normal oceanic crust, which is largely determined by the average mantle temperature [*McKenzie and Bickle*, 1988; *Langmuir et al.*, 1992], we do not even have a theory to explain why the average thickness of continental crust is ~40 km at present. It is thus important to explore the consequences of time-dependent crustal thickness. If the continental crust was thicker in the past [e.g., *England and Bickle*, 1984; *Galer and Mezger*, 1998], the assumption of constant thickness corresponds to the minimum ocean volume [*Korenaga*, 2008c], so it would only increase the net water influx to the mantle. If the crust was thinner, however, the net water flux would decrease, thereby reducing the possibility of a drier mantle in the past and jeopardizing the operation of plate tectonics. Arguments for thinner crust in the past are based on higher-than-present heat production in the crust [e.g., *Fyfe*, 1978], and this idea may be tested quantitatively as follows. First, a steady state geotherm within the continental crust may be calculated as [e.g., *Turcotte and Schubert*, 1982]

$$T(z) = T_s + \frac{A + q_{cm}}{k} z - \frac{A}{2k} z^2, \tag{33}$$

where T_s is the surface temperature, A is a volumetric heat production rate, and q_{cm} is heat flow from the subcontinental mantle. An example for the present-day 40-km-thick crust is given in Figure 13a. The heat production rate and the mantle heat flux are set to 9.8 × 10^{-7} W m^{-3} and 29 mW m^{-2}, respectively, corresponding to the continental heat flux of 14 TW and the continental heat production of 8 TW. The thermal conductivity is known to vary considerably within the crust because of its temperature dependency [e.g., *Whittington et al.*, 2009] but is set to 3 W m^{-1} K^{-1} for the sake of simplicity. If the Hadean continental crust had the same thickness, its Moho temperature would exceed 1000°C (Figure 13a) because crustal heat production was higher than present by a factor of ~4 (Figure 13b). Equation (33) may be solved for crustal thickness so that the Moho temperature does not exceed a given threshold:

$$h_{\max} = \frac{k}{A} \left(\sqrt{\left(\frac{q_{cm}}{k}\right)^2 + \frac{2A}{k}\Delta T} - \frac{q_{cm}}{k} \right), \tag{34}$$

where ΔT is the temperature contrast between the surface and the Moho. The maximum crustal thickness is shown in Figure 13c for three values of ΔT. If the continental Moho cannot be hotter than 800°C (because the lower crust would otherwise melt and flow away), for example, it is difficult to justify a 40-km-thick continental crust before ~2 Ga. In this calculation, the mantle heat flux is assumed to take the present-day value, but it can vary; heat flux from the subcontinental mantle is proportional to the temperature difference across the lithospheric mantle and is inversely proportional to the thickness of the lithospheric mantle. The maximum crustal thickness determined by equation (34), however, is not very sensitive to variations in the mantle

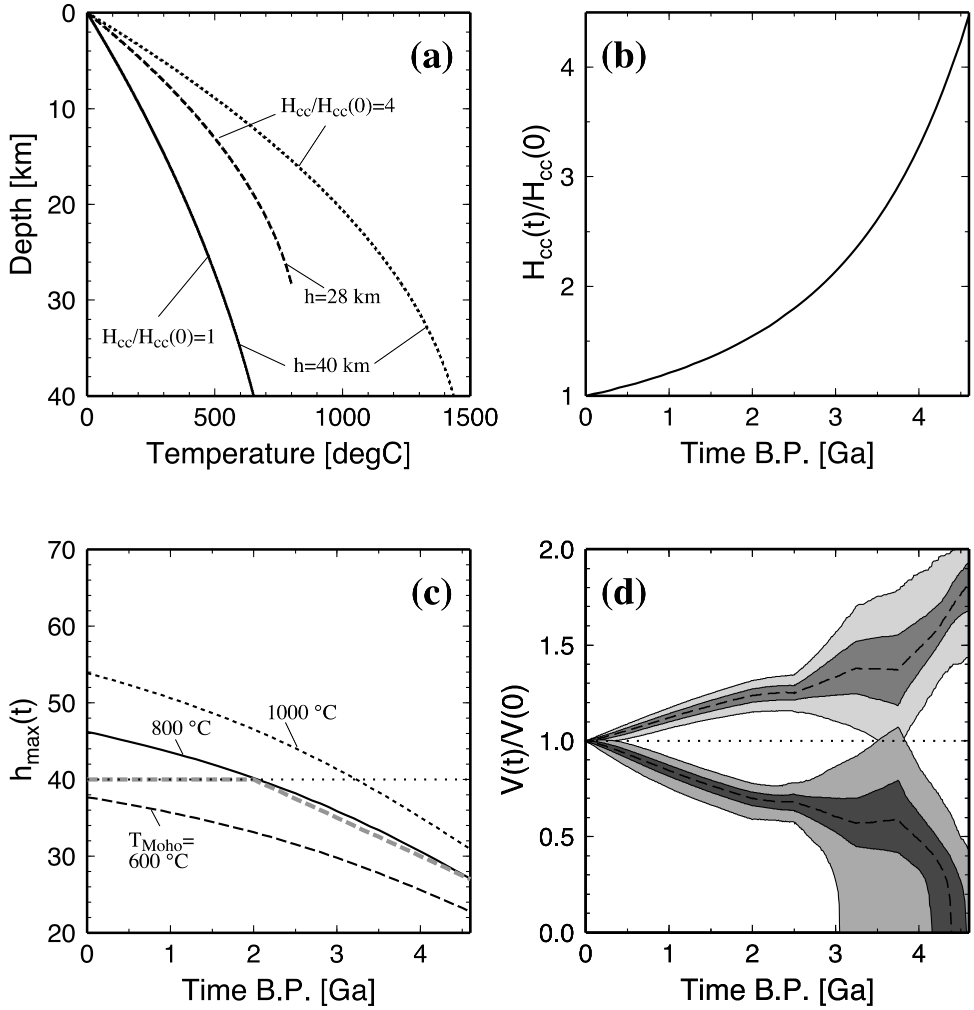

Figure 13. Effect of time-dependent thickness of continental crust on the open-system evolution. (a) Steady state geotherm for continental crust: 40-km-thick crust with present-day heat production (solid) and four times greater heat production (dotted). Moho temperature can be reduced to 600°C if the crust is only 28-km thick (dashed). (b) Variation of crustal heat production with time, based on equations (4) and (5). (c) Maximum crustal thickness based on equation (34) with different threshold Moho temperatures: 600°C (dashed), 800°C (solid), and 1000°C (dotted). Gray dashed line represents equation (35). (d) Same as Figure 9b, but from modeling results with the modified continental fraction of equation (36).

heat flux; 30% higher mantle heat flux, for example, results in only 6–10% decrease in the crustal thickness. Also note that uniform heat production within the crust is assumed in equations (33) and (34) because the once-popular exponential distribution of heat production (i.e., greater heat production at shallower depths) [*Lachenbruch*, 1970] does not seem to be well supported by observations [e.g., *Jaupart and Mareschal*, 2004]. Also, compared at the same total heat production, the uniform distribution results in hotter lower crust than exponential distributions, thus making the crustal thickness calculation here more conservative. For the threshold Moho temperature, 800°C is adopted (as 600°C is too low to explain the present-day crustal thickness; see Figure 13c), and the crustal thickness in the past may be calculated as

$$h_{cc}(t) = \min(40, 50 - 5t), \tag{35}$$

where thickness and time are in km and Ga, respectively. The open-system modeling was repeated with the modified continental fraction defined as

$$F'_{cc}(t) = F_{cc}(t)\frac{h_{cc}(0)}{h_{cc}(t)} \tag{36}$$

in equations (23) and (25). Results are found to be very similar to the original (compare Figure 13d with Figure 9b), suggesting that the possibility of thinner continental crust in the past has only limited influence on the ocean volume calculation.

[40] By contrast, variations in the ridge depth have a substantial impact on the ocean volume. If mid-ocean ridges shallow on a global scale, as in the case of closed-system evolution (Figure 7a), the ocean volume could stay constant despite greater subsidence caused by more sluggish plate tectonics. Theoretical and observational constraints on the

ridge depth in the past are both limited. The Archean oceanic lithosphere, for example, is likely to be more buoyant than the present-day oceanic lithosphere because oceanic crust and depleted mantle lithosphere are both thicker for a hotter mantle [*Korenaga*, 2006], but what is relevant to the ridge depth is the relative buoyancy between oceanic and continental regions. A critical component in this regard is the thickness of subcontinental lithosphere in the past, the consideration of which is usually missing in the literature [e.g., *Nisbet and Fowler*, 1983; *Hynes*, 2001; *Flament et al.*, 2008]. *Galer and Mezger* [1998] argue that the gradual thickening of continental lithosphere with time is unlikely because it would lead to the continuous uplift and exhumation of continents and suggest that the thickness may have been relatively constant. Numerical modeling studies, however, generally show the gradual thinning of continental lithosphere by convective erosion [e.g., *Doin et al.*, 1997; *Shapiro et al.*, 1999]; the continental lithosphere in the Archean could thus have been thick enough to compete with the buoyant oceanic lithosphere. Observational constraints are similarly vague. Based on metamorphic reactions indicated by Archean greenstones in the Pilbara craton, *Kitajima et al.* [2001] suggested that Archean mid-ocean ridges may have been as deep as contemporary ones, and there are also Proterozoic and Archean ophiolite complexes with pillow lavas [e.g., *Dann*, 2001; *Scott et al.*, 1992; *Peltonen et al.*, 1996; *Komiya et al.*, 1999; *Kusky et al.*, 2001; *Furnes et al.*, 2007]. The presence of pillow lavas, however, does not place very quantitative constraints on seafloor depths, and more importantly, it is difficult to estimate a global average ridge depth from these fragmentary Precambrian geological samples. The present-day mid-ocean ridges exhibit considerable depth variations, probably reflecting regional thermal and/or chemical heterogeneities in the source mantle [e.g., *Langmuir et al.*, 1992], so the preservation of a submarine ridge in an ophiolite does not necessarily contradict with an average ridge depth at an subaerial level.

[41] The internal consistency of the open-system evolution as noted in section 3.2 thus plays an important role in interpreting an assemblage of geological data in a dynamically realistic theoretical framework. The continuous operation of plate tectonics at least for the last 3 Ga, as suggested by ophiolites and fossil passive margins with a range of Precambrian ages, demands a positive net water influx to make the mantle drier in the past; otherwise, it is difficult to explain the cooling history of the upper mantle indicated by petrological data. It should be noted, however, that this self-consistency argument depends critically on the scaling laws for plate tectonics, which may be modified or challenged by future theoretical developments. Obtaining new and independent observational constraints on the ocean volume and seafloor depth in the past would thus have a considerable impact on our understanding of the thermal evolution of Earth.

4.3. Net Water Influx, Early Oceans, and Onset of Plate Tectonics

[42] Subducting slabs are hydrated by alteration, and structural water in the oceanic upper crust alone amounts to the water influx of ~9×10^{14} g yr^{-1} [*Ito et al.*, 1983], which is equivalent to subducting the entire ocean in less than 2 billion years. How deeply such subducted water can be distributed in the mantle is not well understood, however, because most of it may quickly return to the surface through arc magmatism [*Jarrard*, 2003], unaffecting the bulk of the mantle. The open-system evolution model presented in section 3.2 suggests the net water flux into the mantle to be ~$2 - 3 \times 10^{14}$ g yr^{-1} (Figure 9b). This continuous hydration of the mantle is entirely opposite to the conventional wisdom that the hydrosphere was formed by the continuous degassing of the mantle [*Rubey*, 1951], but the possibility of a positive net water influx has been suggested repeatedly in the past [e.g., *Fyfe*, 1978; *Ito et al.*, 1983; *Jarrard*, 2003; *Smyth and Jacobsen*, 2006], and the magnitude of net flux estimated in this study is similar to previous estimates based on the water contents of altered oceanic crust and arc magma [*Ito et al.*, 1983; *Jarrard*, 2003] and high-pressure mineral physics data [*Smyth and Jacobsen*, 2006]. Though previous thermal evolution models with water exchange between the surface and the mantle invariably suggest continuous degassing (i.e., negative water influx) [e.g., *McGovern and Schubert*, 1989; *Williams and Pan*, 1992; *Franck and Bounama*, 1997], these models are all based on the assumption of a high present-day Urey ratio (~0.7–0.8), which is inconsistent with the chemical composition model of Earth, and their reconstructed thermal histories are concave upward, being opposite to the actual cooling trend (section 4.1).

[43] As the modeling in this study is formulated with average mantle properties, gradual hydration is assumed to take place over the entire mantle, implying that some part of subducted water can be transported to the deep mantle. Though the dehydration reaction of hydrous minerals in subducting slabs may be limited within the upper mantle [e.g., *Green et al.*, 2010], this by itself does not preclude the deep water cycle because nominally anhydrous minerals can still contain nontrivial amounts of water [*Smyth and Jacobsen*, 2006]. If, however, mantle hydration through time is limited to the upper mantle, the Archean oceans would not be as voluminous as estimated in Figure 9b, and the estimate on net water flux would be reduced by a factor of ~4. The zero-age depth of seafloor during the Proterozoic would also need to be shallower than the present-day to satisfy the freeboard constraint. But in this case, the water content of the lower mantle does not change with time, so the initial water content of the lower mantle at the beginning of subsolidus convection in the Earth history needs to be (somehow) coincide with the present-day water content of the upper mantle. As mentioned in section 2.5, the water content of the MORB-source mantle is on the order of 0.01–0.02 wt%. If the lower mantle beneath a mid-ocean ridge is drier or wetter than this, it would contradict with the petrology of mid-ocean ridge basalts, unless we assume no mass exchange between the upper and lower mantle.

[44] A dry mantle and a voluminous ocean at the beginning of the Earth history both help the initiation of subduction; the former leads to high convective stress, and the latter activates the thermal cracking mechanism. Such situation may even be a natural corollary of the aftermath of a putative magma ocean. Regardless of how efficiently water may have degassed from a solidifying magma ocean, subsequent subsolidus mantle convection in the stagnant-lid regime could quickly process the entire mantle and bring any remaining water in the convecting mantle to the surface [*Fraeman and Korenaga*, 2010]. The existence of oceans and the

operation of plate tectonics in the very early Earth have been suggested by the study of Hadean zircons [e.g., *Mojzsis et al.*, 2001; *Wilde et al.*, 2001; *Valley et al.*, 2005; *Hopkins et al.*, 2010], and though the interpretation of detrital zircons may suffer from nonuniqueness [*Sleep*, 2007], the notion of an early Earth with plate tectonics and oceans is plausible at least on a theoretical ground.

[45] In this study, the continental freeboard is used as an observational constraint to calculate the ocean volume from mantle dynamics, but the success of the thermal evolution modeling may also be interpreted such that the slow but steady mantle hydration regulates the freeboard at the scale of billions of years. When continents rise above the sea level, they can be eroded down, but when continents are globally inundated, there is no obvious mechanism to bring them back to the sea level; crustal thickening by continental collisions is a transient process that takes place only at regional scales. The interaction between the hydrosphere and the solid earth may thus be a key to maintaining a dry landmass over the geologic timescale. In this regard, it is important to understand what controls the net water influx because we still cannot predict it accurately from first principles. *Rüpke et al.* [2004], for example, considered the thermodynamics of subducting slabs and suggested the gradual dehydration of the mantle over the geological time, but it should be noted that their modeling of thermal evolution is based on the assumption that convective heat flux is proportional to internal heat production. This assumption was once popular in the 1970s [e.g., *McKenzie and Weiss*, 1975] but has no physical basis as a number of subsequent studies have shown [e.g., *Schubert et al.*, 1980; *Christensen*, 1985; *Solomatov*, 1995; *Korenaga*, 2008b]. Predicting net water influx as a function of mantle state variables is an important step toward a self-contained theory of mantle convection with predicting power, which would be essential to better understand the evolution of other terrestrial planets including super-Earths [*Korenaga*, 2010b].

[46] **Acknowledgments.** This work was sponsored by the U.S. National Science Foundation under grant EAR-0449517 and Microsoft A. Richard Newton Breakthrough Research Award. The author thanks two anonymous reviewers for comments and suggestions.

References

Abbott, D., and W. Menke (1990), Length of the global plate boundary at 2.4 Ga, *Geology*, *18*, 58–61.
Albarede, F., and R. D. van der Hilst (2002), Zoned mantle convection, *Philos. Trans. R. Soc. London A*, *360*, 2569–2592.
Algeo, T. J., and K. B. Seslavinsky (1995), The Paleozoic world: Continental flooding, hypsometry, and sea level, *Am. J. Sci.*, *295*, 787–822.
Allegre, C. J., A. Hofmann, and K. O'Nions (1996), The argon constraints on mantle structure, *Geophys. Res. Lett.*, *23*, 3555–3557.
Armstrong, R. L. (1981), Radiogenic isotopes: the case for crustal recycling on a near-steady-state no-continental-growth Earth, *Philos. Trans. R. Soc. London A*, *301*, 443–472.
Becker, T. W., C. P. Conrad, B. Buffett, and R. D. Müller (2009), Past and present seafloor age distributions and the temporal evolution of plate tectonic heat transport, *Earth Planet. Sci. Lett.*, *278*, 233–242.
Boyet, M., and R. W. Carlson (2005), ^{142}Nd evidence for early (>4.53 Ga) global differentiation of the silicate Earth, *Science*, *309*, 576–581.
Bradley, D. C. (2008), Passive margins through earth history, *Earth Sci. Rev.*, *91*, 1–26.
Buffett, B. A. (2006), Plate force due to bending at subduction zones, *J. Geophys. Res.*, *111*, B09405, doi:10.1029/2006JB004295.
Buffett, B. A., and A. Heuret (2011), Curvature of subducted lithosphere from earthquake locations in the Wadati-Benioff zone, *Geochem. Geophys. Geosyst.*, *12*, Q06010, doi:10.1029/2011GC003570.
Byerlee, J. (1978), Friction of rocks, *Pure Appl. Geophys.*, *116*, 615–626.
Campbell, I. H. (2003), Constraints on continental growth models from Nb/U ratios in the 3.5 Ga Barberton and other Archaean basalt-komatiite suites, *Am. J. Sci.*, *303*, 319–351.
Carlson, R. L., and H. P. Johnson (1994), On modeling the thermal evolution of the oceanic upper mantle: An assessment of the cooling model, *J. Geophys. Res.*, *99*, 3201–3214.
Christensen, U. R. (1985), Thermal evolution models for the Earth, *J. Geophys. Res.*, *90*, 2995–3007.
Collerson, K. D., and B. S. Kamber (1999), Evolution of the continents and the atmosphere inferred from Th-U-Nb systematics of the depleted mantle, *Science*, *283*, 1519–1522.
Condie, K. C., and V. Pease (Eds.) (2008), *When Did Plate Tectonics Begin on Planet Earth?*, Geol. Soc. of Am., Boulder, Colo.
Conrad, C. P., and B. H. Hager (1999a), Effects of plate bending and fault strength at subduction zones on plate dynamics, *J. Geophys. Res.*, *104*, 17,551–17,571.
Conrad, C. P., and B. H. Hager (1999b), The thermal evolution of an earth with strong subduction zones, *Geophys. Res. Lett.*, *26*, 3041–3044.
Dann, J. C. (2001), Early Proterozoic ophiolite, central Arizona, *Geology*, *19*, 590–593.
Davies, G. F. (2009), Effect of plate bending on the Urey ratio and the thermal evolution of the mantle, *Earth Planet. Sci. Lett.*, *287*, 513–518.
Doin, M.-P., L. Fleitout, and U. Christensen (1997), Mantle convection and stability of depleted and undepleted continental lithosphere, *J. Geophys. Res.*, *102*, 2772–2787.
Durrheim, R. J., and W. D. Mooney (1991), Archean and Proterozoic crustal evolution: Evidence from crustal seismology, *Geology*, *19*, 606–609.
Efron, B. (1982), *The Jackknife, the Bootstrap, and Other Resampling Plans*, Soc. for Ind. and Appl. Math., Philadelphia, Pa.
England, P., and M. Bickle (1984), Continental thermal and tectonic regimes during the Archean, *J. Geol.*, *92*, 353–367.
Eriksson, P. G., R. Mazumder, O. Catuneanu, A. J. Bumby, and B. Ountsche Ilondo (2006), Precambrian continental freeboard and geological evolution: A time perspective, *Earth Sci. Rev.*, *79*, 165–204.
Evans, R. L., G. Hirth, K. Baba, D. Forsyth, A. Chave, and R. Mackie (2005), Geophysical evidence from the MELT area for compositional controls on oceanic plates, *Nature*, *437*, 249–252.
Faul, U. H., and I. Jackson (2007), Diffusion creep of dry, melt-free olivine, *J. Geophys. Res.*, *112*, B04204, doi:10.1029/2006JB004586.
Flament, N., N. Coltice, and P. F. Rey (2008), A case for late-Archaean continental emergence from thermal evolution models and hypsometry, *Earth Planet. Sci. Lett.*, *275*, 326–336.
Fraeman, A. A., and J. Korenaga (2010), The influence of mantle melting on the evolution of Mars, *Icarus*, *210*, 43–57.
Franck, S., and C. Bounama (1997), Continental growth and volatile exchange during Earth's evolution, *Phys. Earth Planet. Inter.*, *100*, 189–196.
Furnes, H., M. de Wit, H. Staudigel, M. Rosing, and K. Muehlenbachs (2007), A vestige of Earth's oldest ophiolite, *Science*, *315*, 1704–1707.
Fyfe, W. S. (1978), The evolution of the Earth's crust: Modern plate tectonics to ancient hot spot tectonics?, *Chem. Geol.*, *23*, 89–114.
Galer, S. J. G., and K. Mezger (1998), Metamorphism, denudation and sea level in the Archean and cooling of the Earth, *Precambrian Res.*, *92*, 389–412.
Gando, A., et al. (2011), Partial radiogenic heat model for Earth revealed by geoneutrino measurements, *Nature Geosci.*, *4*, 647–651.
Green, H. W., W.-P. Chen, and M. R. Brudzinski (2010), Seismic evidence of negligible water carried below 400-km depth in subducting lithosphere, *Nature*, *467*, 828–831.
Gurnis, M. (1993), Phanerozoic marine inundation of continents driven by dynamic topography above subducting slabs, *Nature*, *364*, 589–593.
Hager, B. H. (1984), Subducted slabs and the geoid: Constraints on mantle rheology and flow, *J. Geophys. Res.*, *89*, 6003–6015.
Hargraves, R. B. (1986), Faster spreading or greater ridge length in the Archean?, *Geology*, *14*, 750–752.
Harrison, C. G. A. (1990), Long-term eustasy and epeirogeny in continents, in *Sea-Level Change*, edited by R. R. Revelle, pp. 141–158, Natl. Acad. Press, Washington, D. C.
Harrison, T. M., J. Blichert-Toft, W. Müller, F. Albarede, P. Holden, and S. J. Mojzsis (2005), Heterogeneous Hadean hafnium: Evidence of continental crust at 4.4 to 4.5 Ga, *Science*, *310*, 1947–1950.
Hart, S. R., and A. Zindler (1986), In search of a bulk-earth composition, *Chem. Geol.*, *57*, 247–267.
Hauri, E. H., G. A. Gaetani, and T. H. Green (2006), Partitioning of water during melting of the Earth's upper mantle at H_2O-undersaturated conditions, *Earth Planet. Sci. Lett.*, *248*, 715–734.
Hawkesworth, C. J., and A. I. S. Kemp (2006), Evolution of the continental crust, *Nature*, *443*, 811–817.
Herzberg, C., P. D. Asimow, N. Arndt, Y. Niu, C. M. Lesher, J. G. Fitton, M. J. Cheadle, and A. D. Saunders (2007), Temperatures in ambient

mantle and plumes: Constraints from basalts, picrites, and komatiites, *Geochem. Geophys. Geosyst.*, *8*, Q02006, doi:10.1029/2006GC001390.
Herzberg, C., K. Condie, and J. Korenaga (2010), Thermal evolution of the Earth and its petrological expression, *Earth Planet. Sci. Lett.*, *292*, 79–88.
Hirschmann, M. M. (2006), Water, melting, and the deep Earth H_2O cycle, *Annu. Rev. Earth Planet. Sci.*, *34*, 629–653.
Hirschmann, M. M., C. Aubaud, and A. C. Withers (2005), Storage capacity of H_2O in nominally anhydrous minerals in the upper mantle, *Earth Planet. Sci. Lett.*, *236*, 167–181.
Hirth, G., and D. L. Kohlstedt (1996), Water in the oceanic upper mantle: Implications for rheology, melt extraction, and the evolution of the lithosphere, *Earth Planet. Sci. Lett.*, *144*, 93–108.
Hirth, G., and D. L. Kohlstedt (2003), Rheology of the upper mantle and the mantle wedge: A view from the experimentalists, in *Inside the Subduction Factory*, *Geophys. Monogr. Ser.*, vol. 138, edited by J. Eiler, pp. 83–105, AGU, Washington, D. C.
Hofmann, A. W. (1997), Mantle geochemistry: The message from oceanic volcanism, *Nature*, *385*, 219–229.
Honda, S. (1995), A simple parameterized model of Earth's thermal history with the transition from layered to whole-mantle convection, *Earth Planet. Sci. Lett.*, *131*, 357–369.
Hopkins, M. D., T. M. Harrison, and C. E. Manning (2010), Constraints on Hadean geodynamics from mineral inclusions in >4 Ga zircons, *Earth Planet. Sci. Lett.*, *298*, 367–376.
Howard, L. N. (1966), Convection at high Rayleigh number, in *Proceedings of the Eleventh International Congress of Applied Mechanics*, edited by H. Gortler, pp. 1109–1115, Springer, New York.
Hynes, A. (2001), Freeboard revisited: Continental growth, crustal thickness, change and Earth's thermal efficiency, *Earth Planet. Sci. Lett.*, *185*, 161–172.
Inoue, T., T. Wada, R. Sasaki, and H. Yurimoto (2010), Water partitioning in the Earth's mantle, *Phys. Earth Planet. Inter.*, *183*, 245–251.
Ito, E., D. M. Harris, and A. T. Anderson (1983), Alteration of oceanic crust and geologic cycling of chlorine and water, *Geochim. Cosmochim. Acta*, *47*, 1613–1624.
Jarrard, R. D. (2003), Subduction fluxes of water, carbon dioxide, chlorine, and potassium, *Geochem. Geophys. Geosyst.*, *4*(5), 8905, doi:10.1029/2002GC000392.
Jaupart, C., and J.-C. Mareschal (2004), Constraints on crustal heat production from heat flow data, in Treatise on Geochemistry, vol. 3, *The Crust*, edited by R. L. Rudnick, pp. 65–84, Elsevier, Amsterdam.
Jaupart, C., S. Labrosse, and J.-C. Mareschal (2007), Temperatures, heat, and energy in the mantle of the Earth, in Treatise on Geophysics, vol. 7, *Mantle Dynamics*, edited by G. Schubert, pp. 253–303, Elsevier, Amsterdam.
Jochum, K. P., A. W. Hofmann, E. Ito, H. M. Seufert, and W. M. White (1983), K, U, and Th in mid-ocean ridge basalt glasses and heat production, K/U and K/Rb in the mantle, *Nature*, *306*, 431–436.
Karato, S., and P. Wu (1993), Rheology of the upper mantle: A synthesis, *Science*, *260*, 771–778.
Karato, S., M. S. Paterson, and J. D. FitzGerald (1986), Rheology of synthetic olivine aggregates: Influence of grain size and water, *J. Geophys. Res.*, *91*, 8151–8176.
Kelbert, A., A. Schultz, and G. Egbert (2009), Global electromagnetic induction constraints on transition-zone water content variations, *Nature*, *460*, 1003–1006.
Kelemen, P. B., K. Hanghoj, and A. R. Greene (2004), One view of the geochemistry of subduction-related magmatic arcs, with an emphasis on primitive andesite and lower crust, in Treatise on Geochemistry, vol. 3, *The Crust*, edited by R. L. Rudnick, pp. 593–659, Elsevier, Amsterdam.
Khan, A., A. Kuvshinov, and A. Semenov (2011), On the heterogeneous electrical conductivity structure of the Earth's mantle with implications for transition zone water content, *J. Geophys. Res.*, *116*, B01103, doi:10.1029/2010JB007458.
King, S. D. (1995), Models of mantle viscosity, in *Global Earth Physics: A Handbook of Physical Constants*, pp. 227–236, AGU, Washington, D. C.
Kitajima, K., S. Maruyama, S. Utsunomiya, and J. G. Liou (2001), Seafloor hydrothermal alteration at an Archaean mid-ocean ridge, *J. Metamorph. Geol.*, *19*, 583–599.
Komiya, T., S. Maruyama, T. Masuda, S. Nohda, M. Hayashi, and K. Okamoto (1999), Plate tectonics at 3.8–3.7 Ga: Field evidence from the Isua accretionary complex, southern west Greenland, *J. Geol.*, *107*, 515–554.
Korenaga, J. (2003), Energetics of mantle convection and the fate of fossil heat, *Geophys. Res. Lett.*, *30*(8), 1437, doi:10.1029/2003GL016982.
Korenaga, J. (2006), Archean geodynamics and the thermal evolution of Earth, in *Archean Geodynamics and Environments*, *Geophys. Monogr. Ser.*, vol. 164, edited by K. Benn, J.-C. Mareschal, and K. Condie, pp. 7–32, AGU, Washington, D. C.
Korenaga, J. (2007a), Eustasy, supercontinental insulation, and the temporal variability of terrestrial heat flux, *Earth Planet. Sci. Lett.*, *257*, 350–358.
Korenaga, J. (2007b), Thermal cracking and the deep hydration of oceanic lithosphere: A key to the generation of plate tectonics?, *J. Geophys. Res.*, *112*, B05408, doi:10.1029/2006JB004502.
Korenaga, J. (2008a), Comment on "Intermittent plate tectonics?," *Science*, *320*, 1291–1292, doi:10.1126/science.1155214.
Korenaga, J. (2008b), Urey ratio and the structure and evolution of Earth's mantle, *Rev. Geophys.*, *46*, RG2007, doi:10.1029/2007RG000241.
Korenaga, J. (2008c), Plate tectonics, flood basalts, and the evolution of Earth's oceans, *Terra Nova*, *20*, 419–439.
Korenaga, J. (2009), A method to estimate the composition of the bulk silicate Earth in the presence of a hidden geochemical reservoir, *Geochim. Cosmochim. Acta*, *73*, 6952–6964.
Korenaga, J. (2010a), Scaling of plate-tectonic convection with pseudoplastic rheology, *J. Geophys. Res.*, *115*, B11405, doi:10.1029/2010JB007670.
Korenaga, J. (2010b), On the likelihood of plate tectonics on super-Earths: Does size matter?, *Astrophys. J.*, *725*, 43–46.
Korenaga, J., and S. Karato (2008), A new analysis of experimental data on olivine rheology, *J. Geophys. Res.*, *113*, B02403, doi:10.1029/2007JB005100.
Korenaga, T., and J. Korenaga (2008), Subsidence of normal oceanic lithosphere, apparent thermal expansivity, and seafloor flattening, *Earth Planet. Sci. Lett.*, *268*, 41–51.
Kusky, T. M., J.-H. Li, and R. D. Tucker (2001), The Archean Dongwanzi ophiolite complex, North China craton: 2.505-billion-year-old oceanic crust and mantle, *Science*, *292*, 1142–1145.
Labrosse, S., and C. Jaupart (2007), Thermal evolution of the Earth: Secular changes and fluctuations of plate characteristics, *Earth Planet. Sci. Lett.*, *260*, 465–481.
Lachenbruch, A. H. (1970), Crustal temperature and heat production: Implications of linear heat-flow relation, *J. Geophys. Res.*, *75*, 3291–3300.
Lallemand, S., A. Heuret, and D. Boutelier (2005), On the relationships between slab dip, back-arc stress, upper plate absolute motion, and crustal nature in subduction zones, *Geochem. Geophys. Geosyst.*, *6*, Q09006, doi:10.1029/2005GC000917.
Langmuir, C. H., E. M. Klein, and T. Plank (1992), Petrological systematics of mid-ocean ridge basalts: Constraints on melt generation beneath ocean ridges, in *Mantle Flow and Melt Generation at Mid-Ocean Ridges*, *Geophys. Monogr. Ser.*, vol. 71, edited by J. Phipps Morgan, D. K. Blackman, and J. M. Sinton, pp. 183–280, AGU, Washington, D. C.
Loyd, S. J., T. W. Becker, C. P. Conrad, C. Lithgow-Bertelloni, and F. A. Corsetti (2007), Time variability in Cenozoic reconstructions of mantle heat flow: Plate tectonic cycles and implications for Earth's thermal evolution, *Proc. Natl. Acad. Sci. U. S. A.*, *104*, 14,266–14,271.
Lyubetskaya, T., and J. Korenaga (2007a), Chemical composition of Earth's primitive mantle and its variance: 1. Methods and results, *J. Geophys. Res.*, *112*, B03211, doi:10.1029/2005JB004223.
Lyubetskaya, T., and J. Korenaga (2007b), Chemical composition of Earth's primitive mantle and its variance: 2. Implications for global geodynamics, *J. Geophys. Res.*, *112*, B03212, doi:10.1029/2005JB004224.
Masters, G., G. Laske, H. Bolton, and A. Dziewonski (2000), The relative behavior of shear velocity, bulk sound speed, and compressional velocity in the mantle: Implications for chemical and thermal structure, in *Earth's Deep Interior: Mineral Physics and Tomography From the Atomic to the Global Scale*, *Geophys. Monogr. Ser.*, vol. 117, edited by S. Karato et al., pp. 63–87, AGU, Washington, D. C.
McDonough, W. F., and S.-S. Sun (1995), The composition of the Earth, *Chem. Geol.*, *120*, 223–253.
McGovern, P. J., and G. Schubert (1989), Thermal evolution of the Earth: Effects of volatile exchange between atmosphere and interior, *Earth Planet. Sci. Lett.*, *96*, 27–37.
McKenzie, D., and M. J. Bickle (1988), The volume and composition of melt generated by extension of the lithosphere, *J. Petrol.*, *29*, 625–679.
McKenzie, D., and N. Weiss (1975), Speculations on the thermal and tectonic history of the Earth, *Geophys. J. R. Astron. Soc.*, *42*, 131–174.
McLennan, S. M., and R. S. Taylor (1982), Geochemical constraints on the growth of the continental crust, *J. Geol.*, *90*, 347–361.
Mei, S., and D. L. Kohlstedt (2000), Influence of water on plastic deformation of olivine aggregates: 1. Diffusion creep regime, *J. Geophys. Res.*, *105*, 21,457–21,469.
Mitrovica, J. X., C. Beaumount, and G. T. Jarvis (1989), Tilting of continental interiors by the dynamical effects of subduction, *Tectonics*, *8*, 1079–1094.
Mojzsis, S. J., T. M. Harrison, and R. T. Pidgeon (2001), Oxygen-isotope evidence from ancient zircons for liquid water at the Earth's surface 4,300 Myr ago, *Nature*, *409*, 178–181.

Moresi, L., and V. Solomatov (1998), Mantle convection with a brittle lithosphere: thoughts on the global tectonic styles of the Earth and Venus, *Geophys. J. Int.*, *133*, 669–682.
Nisbet, E. G., and C. M. R. Fowler (1983), Model for archean plate tectonics, *Geology*, *11*, 376–379.
O'Neill, C., A. Lenardic, L. Moresi, T. H. Torsvik, and C.-T. Lee (2007), Episodic Precambrian subduction, *Earth Planet. Sci. Lett.*, *262*, 552–562.
Palme, H., and H. S. C. O'Neill (2004), Cosmochemical estimates of mantle composition, in Treatise on Geochemistry, vol. 2, *The Mantle and Core*, edited by R. W. Carlson, pp. 1–38, Elsevier, Amsterdam.
Parsons, B. (1982), Causes and consequences of the relation between area and age of the ocean floor, *J. Geophys. Res.*, *87*, 289–302.
Parsons, B., and J. G. Sclater (1977), An analysis of the variation of ocean floor bathymetry and heat flow with age, *J. Geophys. Res.*, *82*, 803–827.
Peltonen, P., A. Kontinen, and H. Huhma (1996), Petrology and geochemistry of metabasalts from the 1.95 Ga Jormua ophiolite, northeastern Finland, *J. Petrol.*, *37*, 1359–1383.
Porcelli, D., and K. K. Turekian (2004), The history of platenary degassing as recorded by noble gases, in Treatise on Geochemistry, vol. 4, *The Atmosphere*, edited by R. F. Keeling, pp. 281–318, Elsevier, Amsterdam.
Richard, G., M. Monnereau, and J. Ingrin (2002), Is the transition zone an empty water reservoir? Inferences from numerical model of mantle dynamics, *Earth Planet. Sci. Lett.*, *205*, 37–51.
Richter, F. M. (1985), Models for the Archean thermal regime, *Earth Planet. Sci. Lett.*, *73*, 350–360.
Rose, I. R., and J. Korenaga (2011), Mantle rheology and the scaling of bending dissipation in plate tectonics, *J. Geophys. Res.*, *116*, B06404, doi:10.1029/2010JB008004.
Rubey, W. W. (1951), Geologic history of sea water, *Geol. Soc. Am. Bull.*, *62*, 1111–1148.
Rudnick, R. L., and S. Gao (2004), Composition of the continental crust, in Treatise on Geochemistry, vol. 3, *The Crust*, edited by R. L. Rudnick, pp. 1–64, Elsevier, Amsterdam.
Rüpke, L. H., J. Phipps Morgan, M. Hort, and J. A. D. Connolly (2004), Serpentine and the subduction zone water cycle, *Earth Planet. Sci. Lett.*, *223*, 17–34.
Saal, A. E., E. H. Hauri, C. H. Langmuir, and M. R. Perfit (2002), Vapour undersaturation in primitive mid-ocean-ridge basalt and the volatile content of Earth's upper mantle, *Nature*, *419*, 451–455.
Salters, V. J. M., and A. Stracke (2004), Composition of the depleted mantle, *Geochem. Geophys. Geosyst.*, *5*, Q05B07, doi:10.1029/2003GC000597.
Schubert, G., and A. P. S. Reymer (1985), Continental volume and freeboard through geological time, *Nature*, *316*, 336–339.
Schubert, G., D. Stevenson, and P. Cassen (1980), Whole planet cooling and the radiogenic heat source contents of the earth and moon, *J. Geophys. Res.*, *85*, 2531–2538.
Schubert, G., D. L. Turcotte, and P. Olson (2001), *Mantle Convection in the Earth and Planets*, Cambridge Univ. Press, New York.
Scott, D. J., H. H. Helmstaedt, and M. J. Bickle (1992), Purtuniq ophiolite, Cape Smith belt, northern Quebec, Canada, *Geology*, *20*, 173–176.
Shapiro, S. S., B. H. Hager, and T. H. Jordan (1999), Stability and dynamics of the continental tectosphere, *Lithos*, *48*, 115–133.
Silver, P. G., and M. D. Behn (2008), Intermittent plate tectonics?, *Science*, *319*, 85–88.
Silver, P. G., R. W. Carlson, and P. Olson (1988), Deep slabs, geochemical heterogeneity, and the large-scale structure of mantle convection: Investigation of an enduring paradox, *Annu. Rev. Earth Planet. Sci.*, *16*, 477–541.
Sleep, N. H. (2007), Plate tectonics through time, in Treatise on Geophysics, vol. 9, *Evolution of the Earth*, edited by G. Schubert, pp. 145–169, Elsevier, Amsterdam.
Smith, W. H. F., and D. T. Sandwell (1997), Global sea floor topography from satellite altimetry and ship depth soundings, *Science*, *277*, 1956–1962.
Smyth, J. R., and S. D. Jacobsen (2006), Nominally anhydrous minerals and Earth's deep water cycle, in *Earth's Deep Water Cycle*, *Geophys. Monogr. Ser.*, vol. 168, edited by S. Jacobsen and S. van der Lee, pp. 1–11, AGU, Washington, D. C.
Solomatov, V. S. (1995), Scaling of temperature- and stress-dependent viscosity convection, *Phys. Fluids*, *7*, 266–274.
Solomatov, V. S. (2001), Grain size-dependent viscosity convection and the thermal evolution of the earth, *Earth Planet. Sci. Lett.*, *191*, 203–212.
Spohn, T., and D. Breuer (1993), Mantle differentiation through continental growth and recycling and the thermal evolution of the Earth, in *Evolution of the Earth and Planets*, *Geophys. Monogr. Ser.*, vol. 74, edited by E. Takahashi, R. Jeanloz, and R. Rudie, pp. 55–71, AGU, Washington, D. C.
Spohn, T., and G. Schubert (1982), Modes of mantle convection and the removal of heat from the Earth's interior, *J. Geophys. Res.*, *87*, 4682–4696.
Stein, C. A., and S. Stein (1992), A model for the global variation in oceanic depth and heat flow with lithospheric age, *Nature*, *359*, 123–129.
Tackley, P. J. (2000), Mantle convection and plate tectonics: Toward an integrated physical and chemical theory, *Science*, *288*, 2002–2007.
Takahashi, E., and I. Kushiro (1983), Melting of a dry peridotite at high pressures and basalt magma genesis, *Am. Mineral.*, *68*, 859–879.
Turcotte, D. L., and G. Schubert (1982), *Geodynamics: Applications of Continuum Physics to Geological Problems*, John Wiley, New York.
Valley, J. W., et al. (2005), 4.4 billion years of crustal maturation: Oxygen isotope ratios of magmatic zircon, *Contrib. Mineral. Petrol.*, *150*, 561–580.
Wedepohl, K. H. (1995), The composition of the continental crust, *Geochim. Cosmochim. Acta*, *59*, 1217–1232.
Whittington, A. G., A. M. Hofmeister, and P. I. Nabelek (2009), Temperature-dependent thermal diffusivity of the Earth's crust and implications for magmatism, *Nature*, *458*, 319–321.
Wilde, S. A., J. W. Valley, W. H. Peck, and C. M. Graham (2001), Evidence from detrital zircons for the existence of continental crust and oceans on the Earth 4.4 Gyr ago, *Nature*, *409*, 175–178.
Williams, D. R., and V. Pan (1992), Internally heated mantle convection and the thermal and degassing history of the Earth, *J. Geophys. Res.*, *97*, 8937–8950.
Wise, D. U. (1974), Continental margins, freeboard and the volumes of continents and oceans through time, in *Geology of Continental Margins*, edited by C. A. Burk and C. L. Drake, pp. 45–58, Springer, New York.
Workman, R. K., and S. R. Hart (2005), Major and trace element composition of the depleted MORB mantle (DMM), *Earth Planet. Sci. Lett.*, *231*, 53–72.

J. Korenaga, Department of Geology and Geophysics, Yale University, PO Box 208109, New Haven, CT 06520-8109, USA. (jun.korenaga@yale.edu)